GEOSPHERE

GEOSPHERE, v. 20, no. 3

https://doi.org/10.1130/GES02744.1

13 figures; 1 table; 1 set of supplemental files

CORRESPONDENCE: gasea@wwu.edu

CITATION: Gase, A.C., Bangs, N.L., Van Avendonk, H.J.A., Bassett, D., Henrys, S., Arai, R., Fujie, G. Barnes, P.M., Kodaira, S., Barker, D.H.N., and Okava, D., 2024, Volcanic crustal structure of the western Hikurangi Plateau (New Zealand) from marine seismic reflection imaging: Geosphere, v. 20, no. 3, p. 935-964, https://doi.org/10.1130/GES02744.1

Science Editor: Andrea Hampel Associate Editor: Francesco Mazzarini

Received 17 December 2023 Revision received 4 March 2024 Accepted 18 March 2024

Published online 25 April 2024





This paper is published under the terms of the CC-BY-NC license

© 2024 The Authors

Volcanic crustal structure of the western Hikurangi Plateau (New Zealand) from marine seismic reflection imaging

Andrew C. Gase^{1,2}, Nathan L. Bangs¹, Harm J.A. Van Avendonk¹, Dan Bassett³, Stuart Henrys³, Ryuta Arai⁴, Gou Fujie⁴, Philip M. Barnes⁵, Shuichi Kodaira4, Daniel H.N. Barker3, and David Okava6

Institute for Geophysics, Jackson School of Geosciences, University of Texas at Austin, Austin, Texas 78758, USA

²Geology Department, Western Washington University, Bellingham, Washington 98225, USA

³GNS Science, Post Office Box 30368, Lower Hutt, Wellington 5040, New Zealand

⁴Research Institute for Marine Geodynamics, Japan Institute for Marine-Earth Science and Technology, Yokohama 236-0001, Japan

⁵National Institute for Water & Atmospheric Research (NIWA), Post Office Box 14901, Kilbirnie, Wellington 6140, New Zealand

Department of Earth Sciences, University of Southern California, Los Angeles, California 90089, USA

ABSTRACT

Seamounts and basaltic basement can influence deformation and mass fluxes within subduction zones. We examined seamounts and volcanic units across the western Hikurangi Plateau, near the Hikurangi subduction margin, New Zealand, with seismic reflection images. Volcanism at the Hikurangi Plateau occurred in at least three phases that we attribute to (1) Early Cretaceous large igneous province formation, the top of which is marked by laterally continuous and dipping wedges of reflections that we interpret as lava flows; (2) Late Cretaceous seamounts and volcaniclastics that erupted onto the crust of the Hikurangi Plateau and make up the majority of seamount volume and basement relief; and (3) late-stage, Pliocene volcanics that erupted through and adjacent to Cretaceous seamounts and younger sediments of the northcentral Hikurangi Plateau. The Pliocene volcanoes do not appear to be strongly welded to the plateau basement and may be petit spot volcanoes that are related to the displacement and accumulation of hydrous transition zone melts. Large seamounts and volcaniclastic units are evenly distributed across most of the Hikurangi Plateau near the Hikurangi margin but are absent from the Pegasus Basin. Although faults are imaged throughout the basement of the Pegasus Basin, contemporary normal faulting of the Hikurangi Plateau is uncommon, except for a zone of Quaternary normal faults near the Pliocene volcanics. These trends indicate that the Hikurangi megathrust may be more influenced by volcanic structures in the north and central Hikurangi margin, where plateau rifting and voluminous seamount eruptions have more substantially overprinted the original Early Cretaceous basement.

1. INTRODUCTION

Oceanic large igneous provinces (LIPs) and volcanic plateaus form through enormous eruptions and intrusions of magma within oceanic basins (Coffin

Andrew Gase https://orcid.org/0000-0001-9660-8405

and Eldholm, 1994). Magmatism at LIPs can occur over millions of years in response to a sustained supply of melt from the Earth's mantle (Tarduno et al., 1991; Coffin and Eldholm, 1994). On occasion, LIPs are accompanied by large seamount and volcanic ridge provinces that form contemporarily (Walther, 2003; Homrighausen et al., 2018) or subsequently (Hoernle et al., 2010).

Seamounts represent focused extrusive magmatism and are widespread throughout oceanic basins (Kim and Wessel, 2011). They range in scale from huge constructions that rise several kilometers above the surrounding seafloor (e.g., Louisville Ridge and the Hawaiian-Emperor Seamount Chain), which can cause strong anomalies in the Earth's gravitational field (Smith and Sandwell, 1997; Kim and Wessel, 2011), to small, ~0.1-km-high cones that are detectable only with acoustic sounding (Smith and Cann, 1990; Schwartz et al., 2020). In regions of high-sedimentation, seamounts can be buried. In such cases, they can only be discovered through seismic imaging (von Huene et al., 1997; Han et al., 2018; Frederik et al., 2020; Tan et al., 2022; Gase et al., 2023) or potential field data that can only detect large buried edifices (Smith and Sandwell, 1997).

Both seamounts and LIPs can alter the physical structure and chemistry of subduction zones. Seamounts and LIPs that form from distinct sources cause geochemical anomalies in arc magmas (Timm et al., 2013, 2014; Sano et al., 2016). Because the crust of oceanic LIPs is thicker (8-33 km; Coffin and Eldholm, 1994; Miura et al., 2004; Hochmuth et al., 2019) than normal oceanic crust (~6 km; Van Avendonk et al., 2017; Chen, 1992; Christeson et al., 2019; White et al., 1992), oceanic LIPs are more buoyant and can resist subduction (Cloos, 1993; Almeida et al., 2022). In addition to buoyancy, thickened crust and lithosphere may also increase flexural rigidity and resistance to inelastic yielding, resulting in less slab curvature (Bassett and Watts, 2015; Contreras-Reyes et al., 2021; Bassett et al., 2023). As a result, subduction of LIPs can flatten subducting slabs and enhance orogeny (Liu et al., 2010; Worthington et al., 2012; Horton et al., 2022), sometimes causing tectonic plate reorganizations and changes in magma supply to volcanic arcs (Gulick et al., 2007; Davy et al., 2008; Humphreys, 2009; Liu et al., 2010; Bayona et al., 2012; Wells et al., 2014; Andjić et al., 2018; Riel et al., 2023). Though smaller in size, subducting seamounts can modify the kinematics of faults in accretionary wedges (Dominguez et al.,

2000; Ruh et al., 2016; Morgan and Bangs, 2017; Bangs et al., 2023), promote entrainment and underplating of sediment lenses in their wakes (Sage et al., 2006; Bangs et al., 2023), cause forearc uplift and steepening (Lallemand and Le Pichon, 1987; Park et al., 1999, 2004; Geersen et al., 2015; Marcaillou et al., 2016), erode material from the upper plate (Ranero and von Huene, 2000; Collot et al., 2001; Bangs et al., 2006), influence upper-plate rigidity (Sun et al., 2020; Prada et al., 2023; Bangs et al., 2023), and cause accretion of volcaniclastics and volcanic edifices to the upper plate (Buchs et al., 2009; Clarke et al., 2018; Bonnet et al., 2019, 2020).

The effects of oceanic plateau and seamount subduction on fault-slip processes are controversial (Mochizuki et al., 2008; Bell et al., 2014; Lee et al., 2023). Brittle stick-slip behavior is strongly affected by the frictional properties of rock (e.g., Boulton et al., 2019; Ikari et al., 2011; Kurzawski et al., 2016; Rabinowitz et al., 2018; Shreedharan et al., 2022, 2023), fault material and structural complexity (Fagereng and Sibson, 2010; Skarbek et al., 2012; Scuderi et al., 2017; Fagereng and Beall, 2021), and effective normal stress (Scholz, 1998; Liu and Rice, 2007; Leeman et al., 2016), in which case high-effective normal stresses can promote interseismic fault locking and fast earthquakes. The high-buoyancy of oceanic plateaus and ridges compared to normal oceanic crust has led some to propose that LIP and ridge subduction results in high-effective normal stresses along the megathrust that increase regional fault coupling and produce earthquake asperities (Kelleher and McCann, 1976; Cloos, 1992; Scholz and Small, 1997; Contreras-Reyes and Carrizo, 2011; Myers et al., 2022; Lee et al., 2023). However, geodetic observations along subducting LIPs also show that interseismic coupling can vary along strike (Wallace et al., 2004; Wallace, 2020). Geodetic and seismic observations show that segments where seamounts are common broadly correlate with aseismic creep and slow earthquakes (Mochizuki et al., 2008; Wang and Bilek, 2014; Saffer and Wallace, 2015; Lallemand et al., 2018; Barnes et al., 2020). These zones with rough subducting crust can include portions of subducting oceanic plateaus (Wallace et al., 2004; Chlieh et al., 2011, 2014; Nishimura, 2014), which may contain seamount provinces and exhibit thick volcaniclastic and extrusive upper crustal layers (Walther, 2003; Davy et al., 2008; Bangs et al., 2015; Arai et al., 2017; Gase et al., 2021, 2023).

The Hikurangi Plateau LIP is currently subducting westward beneath the east coast of New Zealand's North Island (Fig. 1A). Here, subducting seamounts and crust of the Hikurangi Plateau could influence along-strike variations in slip behavior of the Hikurangi subduction margin (Wallace et al., 2009; Bell et al., 2010; Barker et al., 2018; Shaddox and Schwartz, 2019; Sun et al., 2020; Barnes et al., 2020; Chesley et al., 2021; Shreedharan et al., 2023, 2022; Gase et al., 2022, 2023; Leah et al., 2022; Bangs et al., 2023). However, seismic imaging investigations of the unsubducted Hikurangi Plateau near the deformation front are sparse, and our knowledge of the geologic nature of its seamounts and upper volcanic crust is restricted to several studies with limited geographic extent (e.g., Davy et al., 2008; Bland et al., 2015; Barnes et al., 2020; Arai et al., 2020; Gase et al., 2021, 2023; Chesley et al., 2021; Bassett et al., 2023). Here, we present >1100 line km of time-migrated,

multichannel seismic (MCS) images spanning the Hikurangi Plateau outboard of the Hikurangi subduction margin (Fig. 1B). We combine these results with previously presented seismic data across the Hikurangi Plateau to assess (1) the stratigraphy and deformation of the subducting basement, (2) the distribution and structure of seamounts, (3) the volcanic evolution of the Hikurangi Plateau, and (4) the possible influence these factors have on processes in the adjacent Hikurangi subduction system. We find stratigraphic evidence of three phases of volcanism spanning the Early Cretaceous to the Pliocene. Spatial variations in crustal structure may be related to the Hikurangi Plateau's history of post-LIP rifting and magmatism.

2. GEOLOGIC BACKGROUND

2.1. Origins and Evolution of the Hikurangi Plateau

The Hikurangi Plateau is an ~4.5 × 10⁵ km² oceanic plateau that formed during the Greater Ontong Java Event (Larson, 1991; Coffin and Eldholm, 1994), a period of widespread LIP activity in the Early Cretaceous (125–120 Ma; Tarduno et al., 1991; Mahoney et al., 1993; Tejada, 2002; Hoernle et al., 2010; Timm et al., 2011; Fig. 2A). Tectonic plate reconstructions from seafloor-spreading magnetic anomalies indicate that the Hikurangi Plateau rifted from the larger Ontong Java and Manihiki plateaus shortly after its formation (ca. 120–110 Ma; Billen and Stock, 2000; Hoernle et al., 2004; Taylor, 2006; Fig. 2B). Mechanisms proposed to have caused the Greater Ontong Java Event include a broad upwelling (i.e., superplume) from the lower mantle (Tarduno et al., 1991; Mahoney et al., 1993; Tejada et al., 1996; Larson, 1997; Hoernle et al., 2010; Timm et al., 2011; Mochizuki et al., 2019; Stern et al., 2020), a large marine meteorite impact (Rogers, 1982; Ingle and Coffin, 2004), and mantle overturning from lithospheric foundering at spreading ridges (Tejada, 2002; Korenaga, 2005; Anderson, 2005).

While the large meteorite impact hypothesis is generally less favored, some factors make the origins of the Greater Ontong Java Event obscure. (1) The Greater Ontong Java Event lacks an obvious trailing hotspot track. The Louisville Ridge has long been proposed as a linked hotspot (Mahoney and Spencer, 1991; Mahoney et al., 1993; Fig. 1A); however, Louisville Ridge seamounts older than ca. 79 Ma have subducted at the Tonga-Kermadec Trench (Koppers et al., 2011), which eliminated a possible direct connection to Ontong Java. A link to the Louisville Ridge also requires true hotspot wander on the order of 8°-19° since the Early Cretaceous (Chandler et al., 2012). (2) Whether the Ontong Java, Manihiki, and Hikurangi plateaus mostly erupted in a deep-water, shallow-water, or subaerial environment is not well established. Mantle upwelling associated with a superplume is expected to cause dynamic topography that would result in shallow-water or subaerial eruptions (Korenaga, 2005). Objections to the mantle superplume hypothesis rely on evidence from volcanic glass volatiles, which indicates that regions of the Ontong Java Plateau erupted at submarine depths >1 km b.s.l. (Roberge et al., 2005). In addition,

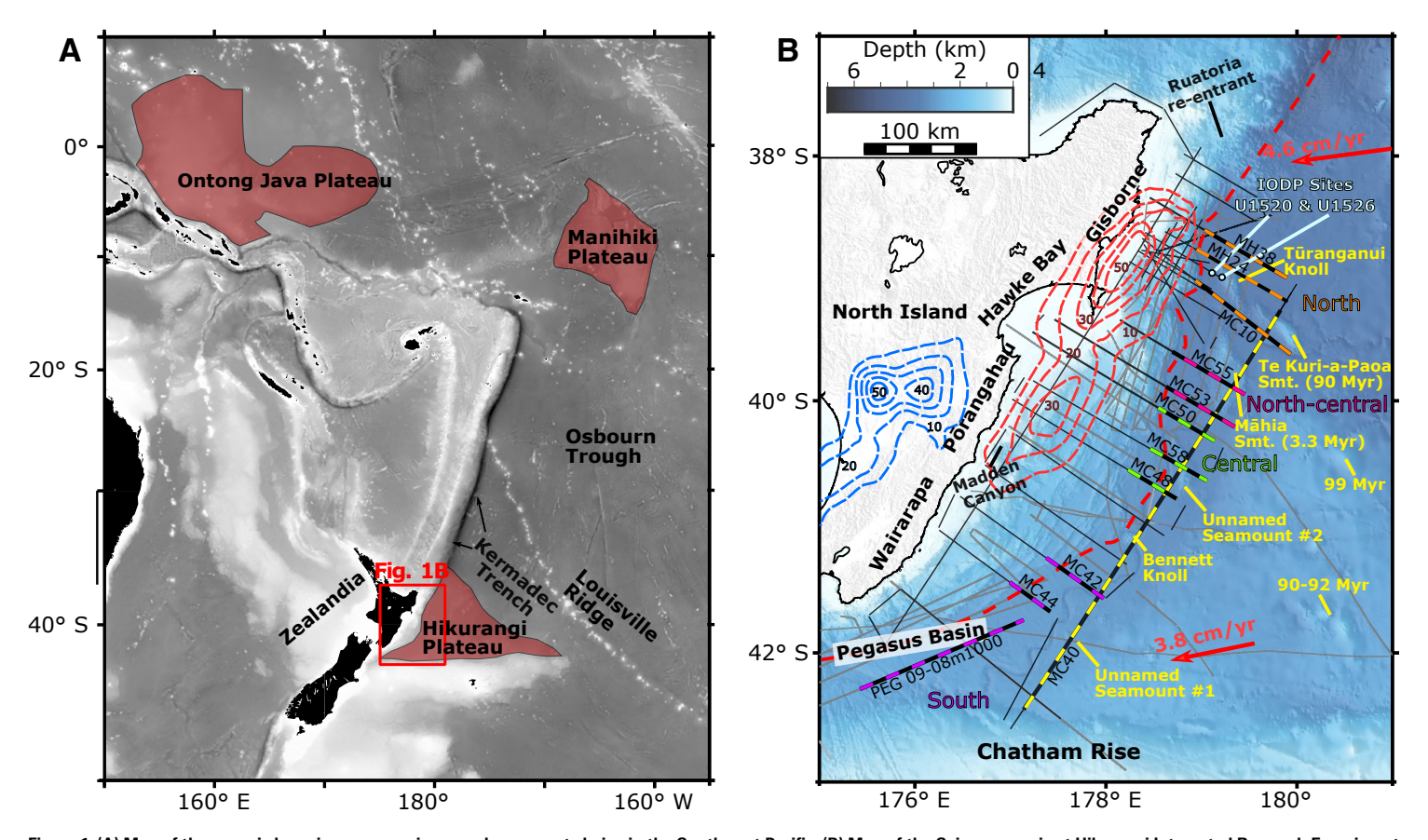
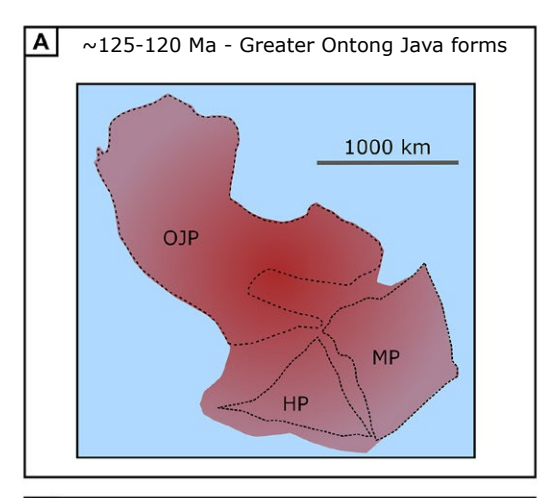


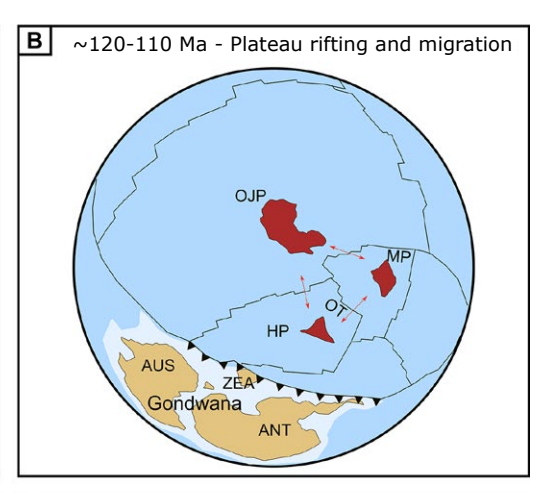
Figure 1. (A) Map of the oceanic large igneous provinces and seamount chains in the Southwest Pacific. (B) Map of the Seismogenesis at Hikurangi Integrated Research Experiment (SHIRE) seismic data (black lines) and past seismic surveys (gray lines). Seismic data presented in this study are marked with colored dashed lines according to region. Red arrows represent the motion of the Pacific Plate relative to the Australian Plate interior (DeMets et al., 2010). Cumulative slow slip (in centimeters) between 2002 and 2014 CE is plotted in red (shallow; i.e., < 20 km) and blue (deep; i.e., >20 km) contours (Wallace, 2020). Names of seamounts and ages of dredged volcanic rocks (Timm et al., 2010; Hoernle et al., 2010) are indicated in yellow. Red dashed line marks the deformation front, including proto-thrust zones (Barnes et al., 2018). Integrated Ocean Discovery Program (IODP) Expedition 375 sites U1520 and U1526 on the Hikurangi Plateau are shown as light blue circles (Wallace et al., 2019; Barnes et al., 2020). Bathymetric data were compiled from SHIRE, National Institute for Water & Atmospheric Research (https://niwa.co.nz/), and Tozer et al. (2019).

deep-water basaltic lava flows of the Ontong Java Plateau are exposed in the Solomon Islands (Tejada, 2002). Thus, some proposed that mantle melting occurred through lithospheric delamination and entrainment of dense, garnet-eclogite—bearing mantle at a mid-oceanic ridge (Korenaga, 2005; Anderson, 2005). However, some evidence of shallow-water eruptions exists. At Ocean Drilling Program Leg 192, Site 1184, on the Ontong Java Plateau, a >337-m-thick volcaniclastic sequence, contains abundant accretionary lapilli and fragments of woody vegetation, which implies that some of the plateau was subaerial

(Thordarson, 2004; White et al., 2004). On the Manihiki Plateau, Deep Sea Drilling Project Leg 33, Hole 317, drilled greenish-black volcaniclastics that likely originated from shallow-marine eruptions (Jenkyns, 1976), and highly vesicular basaltic units that may have erupted subaerially (Jackson et al., 1976). How these diverse paleoenvironments influenced eruption processes and upper crustal structure is not well established.

The Hikurangi Plateau rifted from the Ontong Java and Manihiki plateaus within several million years of its formation (Taylor, 2006; Figs. 2A and 2B).





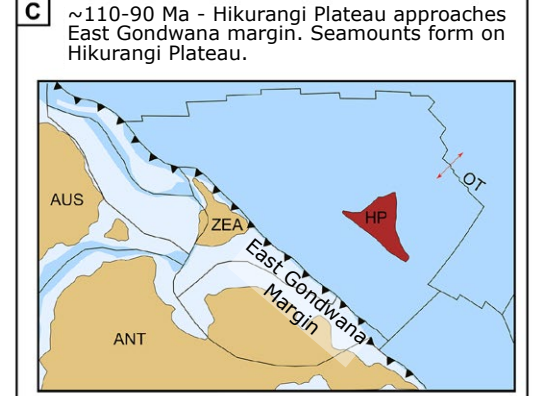




Figure 2. Sketch of the Cretaceous geologic evolution of the Hikurangi Plateau, modeled after Taylor (2006) and van de Lagemaat et al. (2023). (A) Formation of the Greater Ontong Java Event (ca. 125-120 Ma). (B) Ontong Java Plateau (OJP), Manihiki Plateau (MP), and Hikurangi Plateau (HP) rift (ca. 120-110 Ma). (C) Hikurangi Plateau approaches the Gondwana Margin (ca. 110-90 Ma). (D) Hikurangi Plateau collides with the Gondwana margin (ca. 90-79 Ma). Additional acronyms are ANT-Antarctica, AUS-Australia, ZEA-Zealandia, CR-Chatham Rise, and OT-Osbourn Trough.

Rifting occurred along the northeastern edge of the Hikurangi Plateau (Davy and Collot, 2000), and the Hikurangi Plateau is now separated from the Manihiki Plateau by ~3000 km of oceanic crust that formed at the extinct Osbourn Trough spreading center (Billen and Stock, 2000; Fig. 1A). The Rapuhia Scarp is a >400-km-long bathymetric escarpment that has its greatest relief (~1.5 km) near the southern Kermadec Trench (Davy and Collot, 2000; Fig. 3). Seismic images reveal NW-SE-oriented normal fault blocks and a buried yet still abrupt Hikurangi Plateau margin farther east (Davy et al., 2008). The oldest dated rocks on the Hikurangi Plateau are basaltic, gabbroic, and doleritic samples dredged from the Rapuhia Scarp and dated at 118.4-96.3 Ma (Hoernle et al., 2010; Fig. 3B). Wide-angle, controlled-source seismic data and shipboard gravity measurements across the Hikurangi Plateau show that the plateau's crust gradually thins from 11 ± 1 km at the southern Hikurangi Plateau to 78 ± 1 km near the northern rifted margin, which indicates that crustal thinning occurred in response to Cretaceous rifting near ca. 120-115 Ma (Mortimer et al., 2006; Bassett et al., 2023; Fig. 3A).

Southward movement of the Hikurangi Plateau was driven by subduction along the East Gondwana margin (Figs. 2B and 2C), which included both the Chatham Rise and the inner terranes of the modern Hikurangi margin forearc (Bland et al., 2015; Reyners et al., 2017; Crampton et al., 2019; Riefstahl et al., 2020a). Between ca. 90 Ma and 79 Ma, the Hikurangi Plateau collided with the East Gondwana margin (van de Lagemaat et al., 2023; Fig. 2D). This collision was accompanied by slab flattening and slab breakoff (Davy et al., 2008; Riefstahl et al., 2020a) and continental extension throughout the Chatham Rise and Bounty Trough (Reyners et al., 2017; Riefstahl et al., 2020b). Seafloor spreading at the Osbourn Trough and subduction ceased at 79 Ma as plate motion was

D

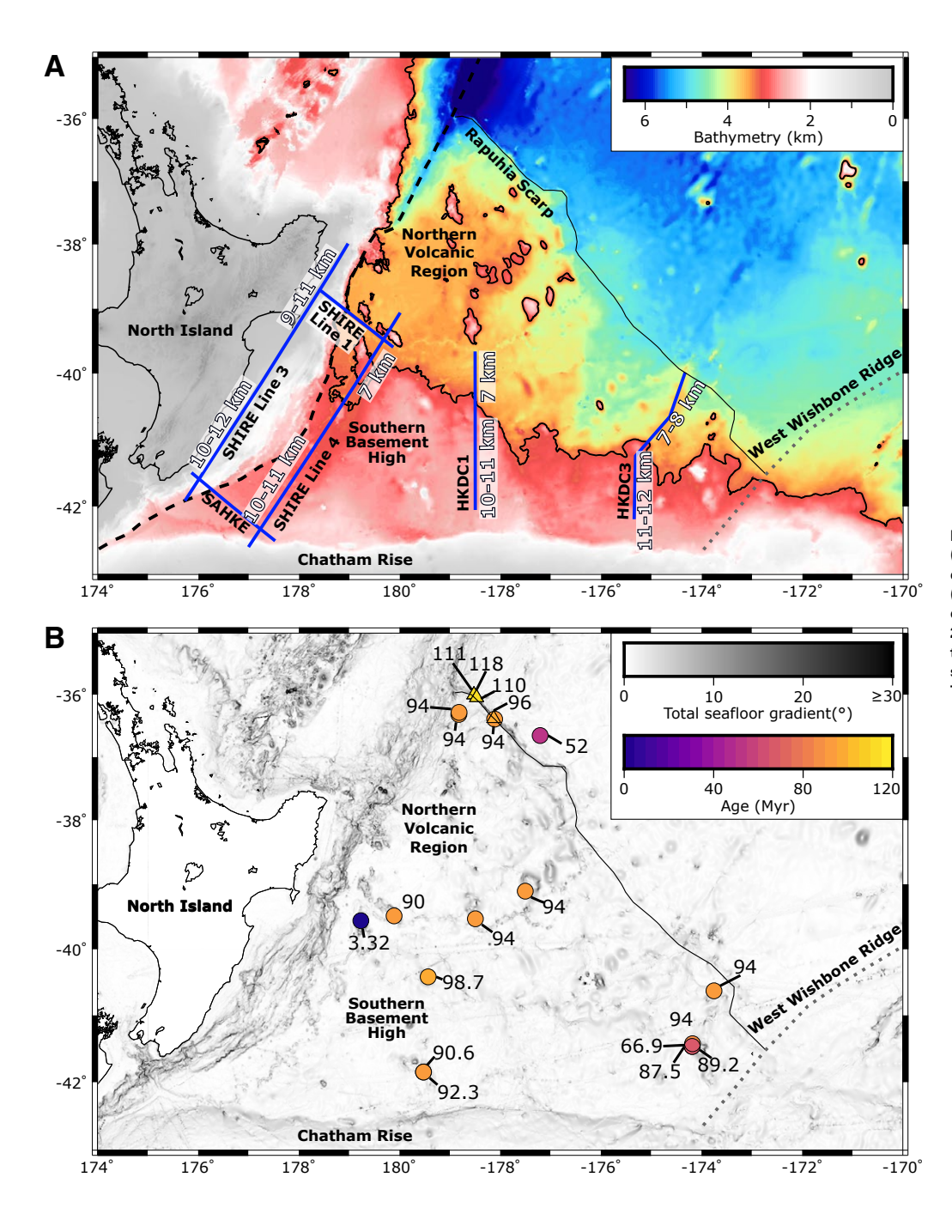


Figure 3. Maps of the Hikurangi Plateau with (A) crustal thickness estimates from the Seismogenesis at Hikurangi Integrated Research Experiment (SHIRE) and HKDC data sets (blue lines; Mochizuki et al., 2019; Gase et al., 2021; Bassett et al., 2022, 2023), and (B) ages of dredged volcanic rocks from the Rapuhia Scarp (triangles) and Hikurangi Plateau seamounts (circles) from Hoernle et al. (2010) and Timm et al. (2010).

transferred to the Pacific-Antarctic Ridge and rifting of Zealandia and Australia from Gondwana (Mortimer et al., 2019; van de Lagemaat et al., 2023).

Basaltic intraplate volcanoes erupted throughout Zealandia and the Hikurangi Plateau at the time of tectonic reorganization (98.7-66 Ma; Hoernle et al., 2020; Fig. 3B). Despite transport through both continental and oceanic LIP lithospheres, Late Cretaceous intraplate volcanoes of the Zealandia continent and the Hikurangi Plateau have signatures of a St. Helena-type HIMU (i.e., high ²³⁸U/²⁰⁴Pb recycled oceanic crust) component that could have been sourced from a broad upwelling of low-density mid-mantle (Hoernle et al., 2010, 2020). The Late Cretaceous intraplate volcanoes on the Hikurangi Plateau erupted as large, >30-km-wide seamounts (Davy et al., 2008; Hoernle et al., 2010). Many of the seamounts have elongated, >50-km-long axes aligned N-S and NW-SE, and steep flanking escarpments, which implies that eruptions took advantage of inherited rift structures in the Hikurangi Plateau basement (Hoernle et al., 2004; Davy et al., 2008; Gase et al., 2023). The peaks of the highest seamounts are broad guyots, which suggests that tidal erosion reworked the original surfaces and that water depths were once ~2.5 km shallower (Davy et al., 2008; Hoernle et al., 2010; Wallace et al., 2019; Allen et al., 2022). In addition, many seamounts are spotted with small (<1-km-wide) volcanic cones (Hoernle et al., 2010; Allen et al., 2022). Later, minor phases of volcanism are indicated by a dredge that recovered ca. 3.2 ± 0.2 Ma Pliocene basanites at Māhia Seamount (Timm et al., 2010; Fig. 3B) and sparse seismic images of sills that intrude Late Cretaceous sediments (Wood and Davy, 1994).

Our current understanding of the Hikurangi Plateau's internal structure and stratigraphy reflects two major phases of volcanism and the subsequent evolution of the plateau (Davy and Wood, 1994; Wood and Davy, 1994; Davy et al., 2008; Bland et al., 2015). From seismic profiles across the central and eastern Hikurangi Plateau, Davy et al. (2008) identified a group of reflectors in the interior of the Plateau (Horizon B) that may separate upper volcaniclastic deposits from the inferred top of the basaltic basement that formed at ca. 125–120 Ma. The location of Horizon B near the Hikurangi subduction zone is not clearly imaged, although some have suggested that it coincides with a diffuse increase in reflectivity and an increase in P-wave velocities ~1.5-3 km below the top of Cretaceous volcanics along the northern Hikurangi margin (Barnes et al., 2020; Gase et al., 2021, 2023). This original plateau basaltic basement is overlain by >1.5 km of volcaniclastics, lavas, and interbedded sediments with slow (1.8-5 km/s) seismic velocities (Davy et al., 2008; Gray et al., 2019; Barnes et al., 2020; Gase et al., 2021, 2023; Bassett et al., 2023) and low-electrical resistivity (Chesley et al., 2021). Both the original basaltic plateau basement and upper volcaniclastics are included in what is commonly referred to as the Hikurangi Plateau basement (Unit HKB). There is widespread evidence of small volcanic edifices and large seamounts that erupted through Unit HKB; some authors suggest that these volcanic features are mantled by a separate thin, highly reflective volcanic basement unit (i.e., VB), but the stratigraphic contact between the HKB and VB units is typically determined based on basement topography rather than a separating stratigraphic horizon (Davy et al., 2008; Barnes et al., 2020). The absolute ages within Unit HKB are not well known or linked to its internal stratigraphy; Unit HKB above Horizon B could include both phases of Early and Late Cretaceous Hikurangi Plateau volcanics and interbedded nonvolcanic sediments, such as carbonates, or HKB above Horizon B could be entirely Late Cretaceous. Davy et al. (2008) suggested the larger mass of the seamounts formed in the Late Cretaceous, but this is speculation without further drilling. Additional seismic profiling may yield new insights into how the seamounts and basement of the Hikurangi Plateau formed.

2.2. Contemporary Subduction of the Hikurangi Plateau

The Hikurangi margin is among the most studied subduction zones on Earth, and it has an actively subducting LIP. Here, the Hikurangi Plateau subducts westward beneath North Island, New Zealand, which uplifts the Hikurangi forearc and produces a shallowly dipping megathrust. Two decades of observations show that the northern and central Hikurangi megathrust is weakly coupled and undergoes shallow slow slip at ~12–18 month recurrence intervals, whereas the southern Hikurangi margin is essentially locked where the megathrust is shallower than ~20–25 km b.s.l. (Wallace et al., 2004; Wallace, 2020). Seafloor pressure measurements demonstrate that these slow slip events extend along the northern and central Hikurangi megathrust from ~20 km depth to the trench (Wallace et al., 2016; Woods et al., 2022). Studies using regional seismic networks and offshore seismic arrays at the northern Hikurangi margin report shallow tectonic tremors and repeating earthquakes during and immediately following shallow slow slip events (Todd and Schwartz, 2016; Todd et al., 2018; Shaddox and Schwartz, 2019).

Proposed factors that contribute to the Hikurangi margin's contrasting along-strike slip behavior are diverse (Wallace et al., 2009; Saffer and Wallace, 2015), and include along-strike variations in the buoyancy of the Hikurangi Plateau (Bassett et al., 2023) and forearc structure (Barnes et al., 2010; Bassett et al., 2014, 2022). Seismic and gravity modeling shows that the southern Hikurangi Plateau is 3-4 km thicker than the northern Hikurangi Plateau (Bassett et al., 2023). This change in along-strike crustal thickness could explain shallower slab-dip throughout the southern Hikurangi seismogenic zone (Williams et al., 2013), and the clockwise rotation of the Hikurangi forearc that influences tectonic stresses and convergence rates (Wallace et al., 2005, 2012). Alternative factors that contribute to the along-strike variation in slip behavior include corresponding variation in Hikurangi Plateau seamounts and volcanic upper crust. Some have proposed that: (1) clay-rich volcaniclastic lithologies along the megathrust are frictionally weak and unable to heal sufficiently during the interseismic period (Shreedharan et al., 2022, 2023); (2) seamounts cause heterogeneous local stress fields that segment the ruptures and allow the slip segments to fail at different rates (Bell et al., 2014; Barker et al., 2018; Sun et al., 2020; Leah et al., 2022); (3) subduction of rough crust causes lithological amalgamation along the megathrust of materials that can support mixed rates of frictional slip (Barnes et al., 2020; Shreedharan et al., 2022; Gase et al., 2022); (4) thick layers of altered volcanic upper crust and seamounts

TABLE 1. DESCRIPTION OF SEISMIC UNITS AS PRESENTED IN FIGURE 4

Seismic facies description	Geologic description	Age range
Subparallel, laterally continuous reflections. Base marked by unconformity (Reflector 5b).	TF—Terrigenous sediments, debris flows, and hemipelagic mudstones.	Middle/early Pleistocene (ca. 2.5 Ma)-present.
Subparallel, laterally continuous reflections, lower strata often faulted. Reflective lower subunit (Sequence Y).	CL—Pelagic sediments that grade from upper marls and calcareous mudstones to lower chalks.	Late Cretaceous (ca. 80 Ma?)-middle/ early Pleistocene (ca. 2.5 Ma).
Subparallel, laterally continuous reflections. Acoustically opaque compared to other units.	MES—Terrigenous and/or hemipelagic sediments from the East Gondwana margin? Never drilled.	Late Cretaceous (ca. 90 Ma)-Late Cretaceous (ca. 80 Ma?).
Upper portion contains irregular, sometimes subparallel, <2-km- long reflectors. Top of occasionally visible band of subparallel reflectors is interpreted as Horizon B. Becomes more transparent below Horizon B.	HKB—Hikurangi Plateau basement. Heavily altered volcaniclastic facies and basaltic debris flows where drilled. Could contain interbedded nonvolcanic sediments. Lower subunit below Horizon B may represent Early Cretaceous basaltic basement.	Early Cretaceous (ca. 125 Ma)-Late Cretaceous (ca. 90 Ma).

host large fluid reservoirs that promote fluid overpressures at the megathrust (Chesley et al., 2021; Gase et al., 2023); and (5) fluid-rich, weak materials in the upper plate are entrained behind or in front of subducting topography (Bell et al., 2010; Bangs et al., 2023). A more complete seismic stratigraphy of the Hikurangi Plateau's volcanic units outboard of the subduction zone will help to determine the structures and lithologies that can be expected within the subducted Hikurangi Plateau.

3. SEISMIC REFLECTION DATA AND INTERPRETATION STRATEGY

We present time-migrated seismic reflection data that were acquired in 2017, during the Seismogenesis at Hikurangi Integrated Research Experiment (SHIRE). All SHIRE MCS data were acquired with a tuned 36 air-gun array with a total source volume of 6600 in3. We recorded 14 s of data per shot at a 2 ms sampling interval on a 12.6-km-long, 1008 channel solid-state hydrophone streamer towed 10 m b.s.l. The SHIRE seismic data span the entire length of the Hikurangi subduction margin (Fig. 1B), which provides an exceptional opportunity to examine the crustal structure of the western Hikurangi Plateau along strike. The complete seismic experiment includes 18 margin-perpendicular seismic reflection profiles that traverse the incoming plate and offshore forearc (Fig. 1B) and several additional lines that parallel the trench. Presentations of SHIRE seismic data can be found in other publications (Gase et al., 2021, 2022; Bassett et al., 2022, 2023; Wang et al., 2023). We focus on segments of 11 SHIRE MCS lines on the Hikurangi Plateau, outboard of the deformation front. The longest of these lines, MC40, is collocated with the 460-km-long, wide-angle SHIRE Line 4 and presented alongside a seismic velocity model in Bassett et al. (2023). The 10 other SHIRE MCS profiles presented here are oriented perpendicular to the deformation front. In our analysis, we include an additional time-migrated image (PEG09-08m1000) located in the Pegasus Basin that was originally published by Bland et al. (2015).

Our MCS processing strategy is identical to time-migrated images of the Hikurangi forearc presented in Gase et al. (2022). The seismic data were (1) resampled to 4 ms, (2) filtered with a 1-D trapezoidal band-pass filter to reduce oceanic swell noise (ramp frequencies 1–2 and 60–100 Hz), and (3) gain adjusted for trace balancing and spherical divergence (t^2). Traces were sorted into 6.25-m-wide common-midpoint (CMP) bins. We attenuated multiples with a combination of surface-related multiple elimination in the shot domain (SRME) followed by radon filtering in the CMP domain. Stacking velocities were picked iteratively at 250–500 CMP intervals (~1.56–3.12 km) to flatten common image gathers from Kirchhoff pre-stack time migration. After migration, common image gathers were muted and stacked.

We combined these SHIRE seismic images with previously published single-channel seismic and MCS data to map the top of the Hikurangi Plateau basement across the margin. The source and receiver characteristics of the prior surveys used here can be found in Table S1 in the Supplemental Material. We also used seismic reflection data from SHIRE turn lines for horizon mapping. We manually selected two-way traveltimes along the top of the Hikurangi Plateau volcanics (Unit HKB). Horizon picks were converted to apparent depth with a 1-D velocity function from sediments in the Pegasus Basin (Mochizuki et al., 2019). This approach does not account for lateral variations in seismic velocity due to lithological variations in the sedimentary units, but it allows for a more intuitive interpretation of basement depth across the Hikurangi Plateau than two-way traveltime. We gridded horizon picks with a nearest-neighbor function, nearneighbor, from Generic Mapping Tools 6.0 (Wessel et al., 2019), which computes gridded values from the weighted mean of nearest picks within a defined search radius. A search radius of 40 km was used because it is the approximate distance between margin-perpendicular SHIRE seismic profiles.

We adopted a seismic stratigraphy framework from Gase et al. (2022; Table 1), which is based on work by several authors (Bland et al., 2015; Barnes et al., 2020) and is correlated with logged stratigraphy at Integrated Ocean Discovery Program (IODP) Expedition 375, Site U1520 (Fig. 1B; Barnes et al., 2019). The lack of widespread well-ties warrants caution when interpreting lithologies

¹Supplemental Material. Uninterpreted seismic reflection images and seismic reflection survey details. Please visit https://doi.org/10.1130/GEOS.S.25505380 to access the supplemental material, and contact editing @geosociety.org with any questions.

and ages, particularly in the southern Hikurangi Plateau. The top of Cretaceous volcanics (Unit HKB, >90 Ma) is well established in other publications (Davy et al., 2008; Barnes et al., 2020; Bassett et al., 2023) and can be easily distinguished from younger sediments due to seamount topography, high-amplitudes, and more chaotic reflection facies (Fig. 4). We tentatively interpret Horizon B in seismic profiles as a subhorizontal zone of increased reflection strength within Unit HKB. In addition to the Hikurangi Plateau's volcanic stratigraphy, we interpret three key, previously defined sedimentary units that were deposited throughout the volcanic development of the plateau and correspond to major lithologic contrasts in the subduction sedimentary inputs, and have clear bounding horizons (Davy et al., 2008; Barnes et al., 2010, 2020; Plaza-Faverola et al., 2012; Bland et al., 2015; Crutchley et al., 2020; Gase et al., 2022; Fig. 4). The oldest sedimentary plateau cover unit, Mesozoic sediments (Unit MES) (ca. 90-80 Ma), has weak seismic amplitudes, and it is composed of Late Cretaceous siliciclastic sediments that continue into the extinct Gondwana accretionary wedge of the Chatham Rise (Plaza-Faverola et al., 2012; Bland et al., 2015;

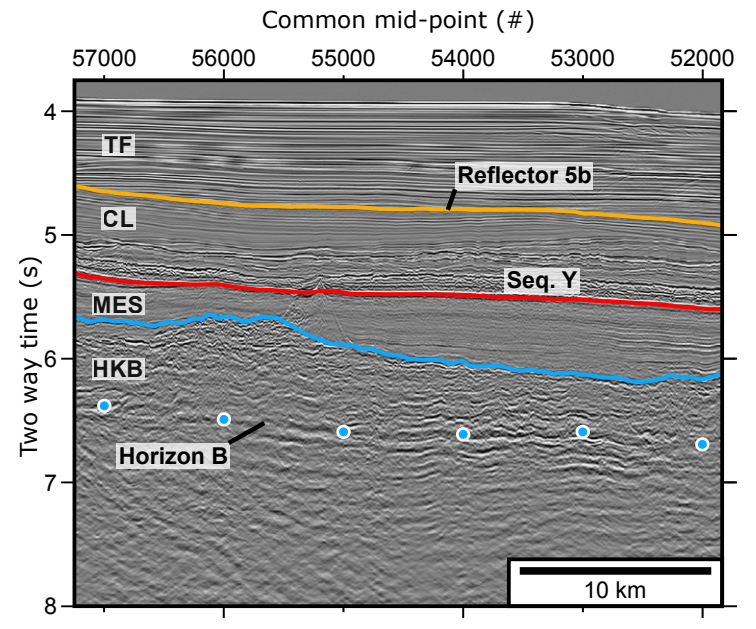


Figure 4. Portion of the Seismogenesis at Hikurangi Integrated Research Experiment Line 4/MC40 with seismic horizon descriptions indicated in Table 1, assuming continuity of comparable units drilled at Integrated Ocean Discovery Program Site U1520 (Barnes et al., 2019, 2020; Fig. 1B). Stratigraphic horizons include the Reflector 5b unconformity (yellow line) that separates trench-fill hemipelagic sediments (TF) from calcareous pelagic sediments (CL), the horizon that separates Sequence Y (Seq. Y) from Unit MES (Mesozoic sediments; red line), the top of Unit HKB (Hikurangi Plateau basement; blue line), and Horizon B (blue dots). Vertical exaggeration is 5.2 at 2.5 km/s.

Mochizuki et al., 2019; Gase et al., 2022). This unit is overlain by pelagic sediments with relatively high calcite concentrations (Unit CL; ca. 80–2.5 Ma; Barnes et al., 2020). The oldest age of Unit CL near the trench is not well established; its lower sequence is strongly reflective and primarily comprised of nannofossil chalks (Sequence Y) that could be Late Cretaceous to Paleocene (Davy et al., 2008; Barnes et al., 2010). Where drilled at the northern Hikurangi margin at IODP Site U1520, Unit CL grades upwards from lower Paleocene nannofossil chalks to marls with interbedded debris-flow deposits (Barnes et al., 2019). The top of Unit CL is bounded by a regional unconformity (Reflector 5b) that separates Quaternary marls and debris flows from upper hemipelagic trench-wedge facies (Unit TF; present–2.5 Ma) at the northern Hikurangi margin (Barnes et al., 2019). The age of the Reflector 5b horizon may be diachronous and is not well constrained elsewhere.

4. RESULTS

We present several seismic profiles in geographic order. We first present MC40 (SHIRE Line 4), which approximately parallels the deformation front. Then we present seismic profiles grouped by location along the margin (i.e., north, north-central, central, and south). We focus on the characteristics of the unsubducted Hikurangi Plateau basement, seamounts, and volcaniclastic cover (Unit HKB), and primary volcanic features within the sedimentary cover of the plateau. Other publications present the seismic stratigraphy and structure of the Hikurangi forearc (Barker et al., 2009; Bell et al., 2010; Pedley et al., 2010; Barnes et al., 2010; Plaza-Faverola et al., 2012, 2016; Bland et al., 2015; Ghisetti et al., 2016; Crutchley et al., 2020; Davidson et al., 2020; Arnulf et al., 2021; Gase et al., 2022, 2021; Bassett et al., 2022; Bangs et al., 2023), incoming sedimentary units (Bassett et al., 2023; Wood and Davy, 1994; Davy et al., 2008; Plaza-Faverola et al., 2012; Bland et al., 2015; Barnes et al., 2018, 2020; Crutchley et al., 2020; Gase et al., 2021, 2022; Wang et al., 2023), and the geophysical properties of the Hikurangi Plateau basement in detail (Davy et al., 2008; Henrys et al., 2013; Mochizuki et al., 2019; Gray et al., 2019; Barnes et al., 2020; Stern et al., 2020; Herath et al., 2020; Arai et al., 2020; Gase et al., 2021, 2023; Chesley et al., 2021; Bassett et al., 2022, 2023; Bangs et al., 2023).

4.1. SHIRE Line 4/MC40 along Strike

SHIRE Line 4 parallels the strike of the Hikurangi subduction zone. This line was first presented alongside wide-angle seismic data and gravity data in Bassett et al. (2023). Bathymetric and seismic reflection data along this line reveal five prominent seamounts that are spaced ~50–75 km apart (Fig. 5). The sedimentary cover thins substantially from north to south along Line 4, from ~1.5 s to ~2.8 s at the base of the Chatham Rise (all thicknesses are reported in two-way traveltime). The largest seamounts in the southern Hikurangi margin are almost completely buried and hidden from seafloor bathymetry (Fig. 5). Three of the

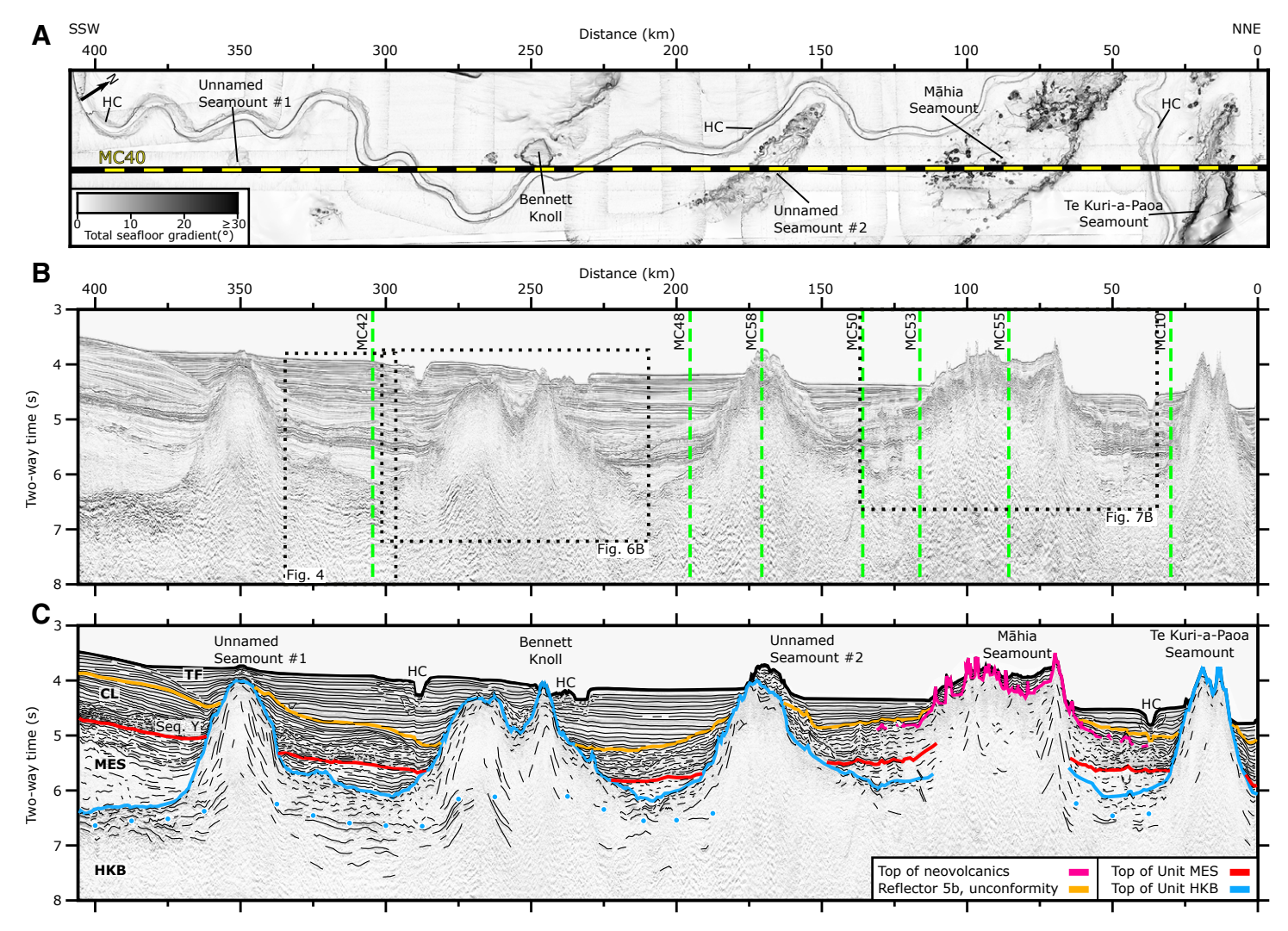


Figure 5. (A) Line-adjacent bathymetry gradient map, (B) pre-stack time-migrated image, and (C) interpretation of the Seismogenesis at Hikurangi Integrated Research Experiment Line 4/MC40. (B) Crossline lines are noted by vertical green dashed lines. (C) Stratigraphic horizons include the top of late-stage volcanics (magenta line), the Reflector 5b unconformity (yellow line), which separates trench-fill hemipelagic sediments (TF) from calcareous pelagic sediments (CL), the horizon that separates Sequence Y (Seq. Y) from Unit MES (Mesozoic sediments; red line), the top of Unit HKB (Hikurangi Plateau basement; blue line), and Horizon B (blue dots). HC—Hikurangi Channel. Vertical exaggeration is 15.2 at 2.5 km/s.

seamounts, including Unnamed Seamount #1, Unnamed Seamount #2, and Te Kuri-a-Paoa Seamount, have narrower in-profile basal widths of ~35–50 km, whereas Bennett Knoll and Māhia Seamount are broader (~75 km wide). All of these seamounts rise ~2–2.5 s (~2–3 km) above the regional basement topography, which slopes gently from ~6 s in the north to ~6.5 s in the south.

The strength and depth of reflections within Unit HKB vary along SHIRE Line 4 (Fig. 5). At the southern end of the profile (~375–400 km), the top of Unit HKB is an ~0.5-s-thick package of relatively strong, subparallel reflections. Similar packages of strong reflections are observed on the opposite side of Unnamed Seamount #1 between ~300–340 km at ~0.6 s below the top of Unit HKB. These strong, laterally continuous horizons within Unit HKB are similar to the top of Horizon B, which Davy et al. (2008) designated as the acoustic basement on the central Hikurangi Plateau. The reflections associated with Horizon B can be traced into the cores of Unnamed Seamount #1 and Bennett Knoll, as strong, outward-dipping reflections that approximately parallel the seamounts' topography. Faster seismic velocities (~4–6 km/s) in the seamounts as reported by Bassett et al. (2023) will cause seamount interior reflections to arrive sooner than adjacent subbasin reflectors. Strong Horizon B reflections are not observed in the northern half of the profile, and reflections within the interiors of the three northern seamounts are more diffuse and discontinuous.

The three southernmost seamounts and Te-Kuri-a-Paoa Seamount have similar internal structures and outer surface geometries. Flat-top regions (i.e., guyots) on some of these seamounts (e.g., Bennett Knoll and Te-Kuri-a-Paoa Seamount) are the result of wave erosion from a shallow-marine environment and indicate at least 2.5 km of subsidence since 90 Ma (Figs. 5A and 6A). Above Horizon B, these seamounts are composed of ~0.5-1.5-s-thick wedges of subparallel, inclined reflections that typically dip with the seamounts' topography, like those observed on the southern flank of Bennett Knoll (Fig. 6). These inclined, layered reflections resemble massive lava flows observed at the Shatsky Rise (Sager et al., 2013) and Manihiki Plateau (Pietsch and Uenzelmann-Neben, 2015). Other regions along the flanks of these four seamounts, including the northern flank of Bennett Knoll (Fig. 6D), exhibit more chaotic reflection patterns that may suggest volcanic mass wasting during or after eruptions (Leslie et al., 2002). The top surfaces of these four seamounts exhibit rare (<2-km-wide) volcanic cones, linear fissures, and fractures, but they are mostly smooth, with truncated reflections that are consistent with post-volcanic wave planation (Davy et al., 2008; Figs. 5A and 6A).

In SHIRE Line 4/MC40, the structure of Māhia Seamount is different from that of the other four seamounts (Figs. 5 and 7). The tops of units HKB and MES can be traced toward the flanks of the seamount, where they are lost in a zone of discontinuous reflections in the seamount's interior (Fig. 7B). An ~60-km-long, N–S-oriented ridge with steeply inclined interior reflections on Māhia Seamount's northern flank (Figs. 7A and 7B, CMP 15,000–15,500) appears to contain lava flows of a similar nature to those observed at Bennett Knoll (Fig. 6). The upper volcanic surface of Māhia Seamount is much rougher than that of other large seamounts and is pocked with small cones (Fig. 7A). Highly reflective horizons underlain by chaotic reflections emanate from the

peak of the seamount and are onlapped by Unit TF and younger strata of Unit CL. Based on the early Pleistocene age of the top of Unit CL, Reflector 5b, at IODP Site U1520 (Barnes et al., 2020), the bright horizons emanating from Māhia Seamount are likely a lava or volcaniclastic fan from the 3.2 ± 0.2 Ma eruptions documented by Timm et al. (2010), which we hereafter refer to as neovolcanics. Prominent scarps of the northeastern flank of Māhia Seamount may have sourced some of these deposits (Fig. 7A). Some high-amplitude horizons are cone or mound shaped. The amplitudes of reflections within Unit CL are reduced beneath these highly reflective units, and some regions exhibit pull-up, presumably from lavas that are seismically faster than adjacent sediments (Fig. 7C). Beneath these reflective neovolcanic units, within Unit MES, we observe cuspate and flat-lying reflectors; we interpret these features to be magmatic sills. A prominent ~3-km-wide, cup-shaped reflector transgresses Unit MES, ~15-20 km northeast of Māhia Seamount, at ~5.8 s and between CMPs 11,000 and 11,500 (Figs. 7B and 7D). An ~3-km-wide anticline in the sediments directly above this sill may be a forced fold (Thomson and Schofield, 2008) caused by intrusion of this sill, although some apparent dip in the overlying sediments may be due to velocity pull-up or differential compaction. Unit CL is heavily deformed by polygonal faults, and faulting induced by sill intrusion and polygonal faulting cannot be differentiated easily.

4.2. North Profiles Offshore Gisborne

Seismic profiles MH38, MH24, and SHIRE Line1b/MC10 are oriented perpendicular to the margin (Fig. 8). In the northernmost profiles (MH38 and MH24), Unit TF includes massive debris avalanche deposits from the Ruatoria debris avalanche that initiated ~50–75 km to the north and thins southward (Figs. 8A and 8B). A small (~1-km-wide) neovolcanic mound is observed beneath the Reflector 5b unconformity at ~68 km from the deformation front in seismic profile MH38 (Fig. 8A). This neovolcanic mound is located within the upper strata of Unit CL, similar to neovolcanics observed near Māhia Seamount, which lies ~50 km to the southwest (Figs. 5 and 7). We observe no faults with significant throw in the Hikurangi Plateau basement, nor any active subduction-related bend faults that would offset the sediment cover.

Three large seamounts are observed across this segment of the margin (Fig. 8). Tūranganui Knoll is oriented NNW–SSE and is prominent (~2 s high) in the central portions of seismic profiles MH38 (30–50 km) and MH24 (~15–60 km; Figs. 8A and 8B). Small, buried (~0.75-s-high) volcanic cones in the center of profile MC10 are associated with Tūranganui Knoll (Fig. 8C). The western flank of an unnamed, largely buried volcanic edifice rises ~1 s above a basement low at the southeast end of profile MH38 (Fig. 8A). Puke Knoll rises above the regional volcanic basement (~2 s high) at the deformation front of SHIRE Line 1b/MC10 (Fig. 8C). Small volcanic cones and a basement high at the deformation front of profiles MH38 and MH24 also appear to be a continuous ridge of volcanism associated with Puke Knoll (Figs. 8A and 8B), which 3-D seismic data show is a NNW–SSE-oriented linear volcanic edifice (Gase et al., 2023).

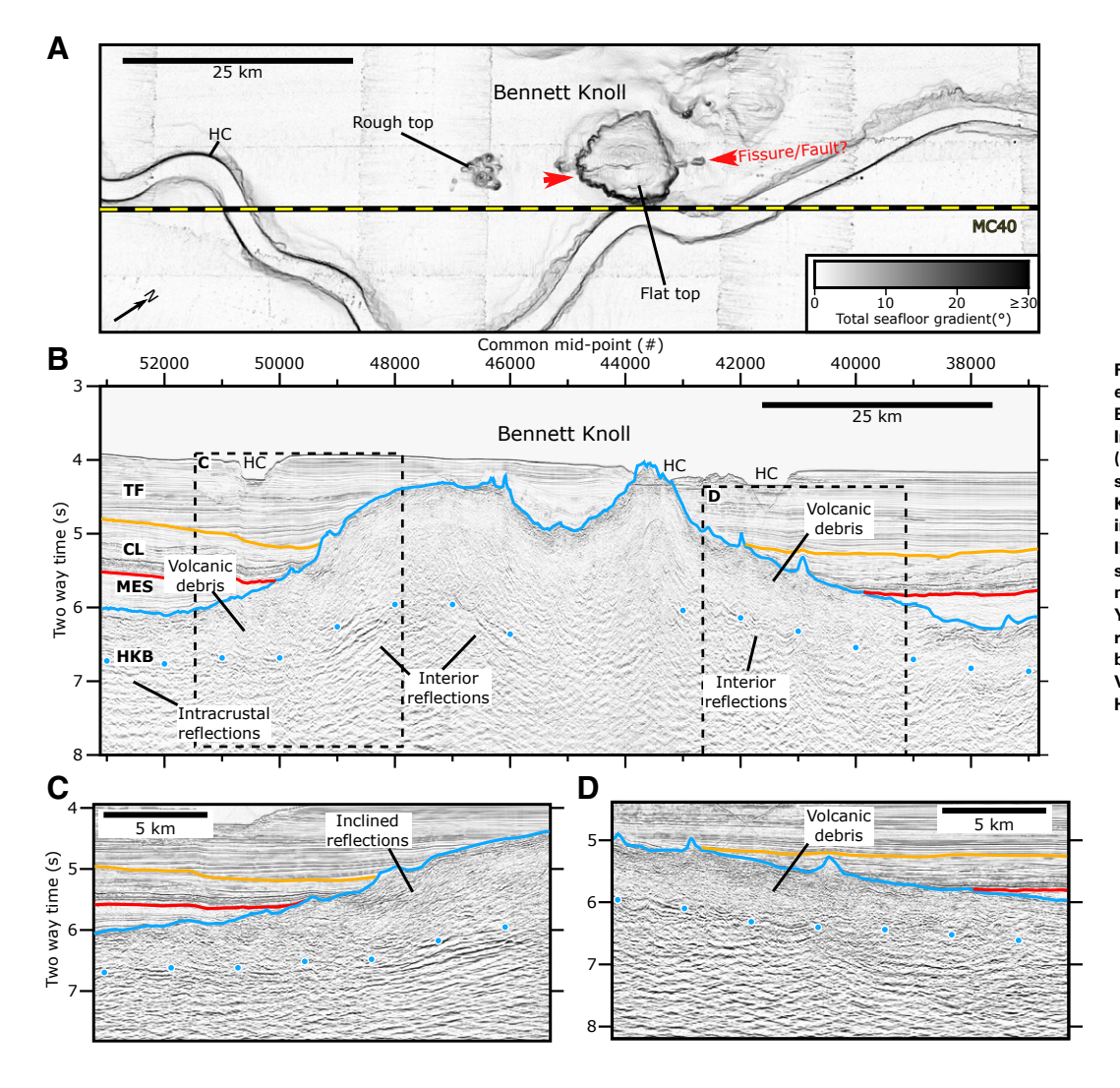


Figure 6. (A) Line-adjacent bathymetric gradient map. (B) Pre-stack time-migrated image of Bennett Knoll from Seismogenesis at Hikurangi Integrated Research Experiment Line 4/MC40 (Fig. 5). (C) Enlarged view of Bennett Knoll's southern flank. (D) Enlarged view of Bennett Knoll's northern flank, Stratigraphic horizons include the Reflector 5b unconformity (yellow line), which separates trench-fill hemipelagic sediments (TF) from calcareous pelagic sediments (CL), the horizon that separates Sequence Y (Seq. Y) from Unit MES (Mesozoic sediments; red line), the top of Unit HKB (Hikurangi Plateau basement; blue line), and Horizon B (blue dots). Vertical exaggeration is 6.5 at 2.5 km/s. HC-Hikurangi Channel.

The upper surfaces of Tūranganui Knoll and Puke Knoll are roughened by small volcanic cones. Tūranganui Knoll has a broad flat top with truncated volcanic clastic reflections, an irregular cover veneer of sediment drifts, and younger volcanic cones that imply resurgent volcanism after erosion and subsidence (Wallace et al., 2019; Allen et al., 2022; Fig. 8).

Reflections within Unit HKB are observed across the three profiles (Fig. 8). The flanks of large seamounts, such as Puke and Türanganui knolls, contain wedges of inclined reflectors that we interpret as lava flows, and zones

of chaotic reflections that we suspect are volcaniclastic debris (Barnes et al., 2020; Gase et al., 2023). Some of the adjacent basins contain reflectors that appear to emanate from the larger volcanic edifices, which implies that broad regions of the northern Hikurangi Plateau are covered by volcaniclastic debris and lavas from large seamounts nearby. We do not observe an unequivocal Horizon B. However, bands of strong reflections that may be related to Horizon B are observed ~1–1.5 s below the top of Unit HKB near Tūranganui Knoll (Figs. 8A and 8B; Barnes et al., 2020) and ~0.75–1 s below the top of Unit HKB near

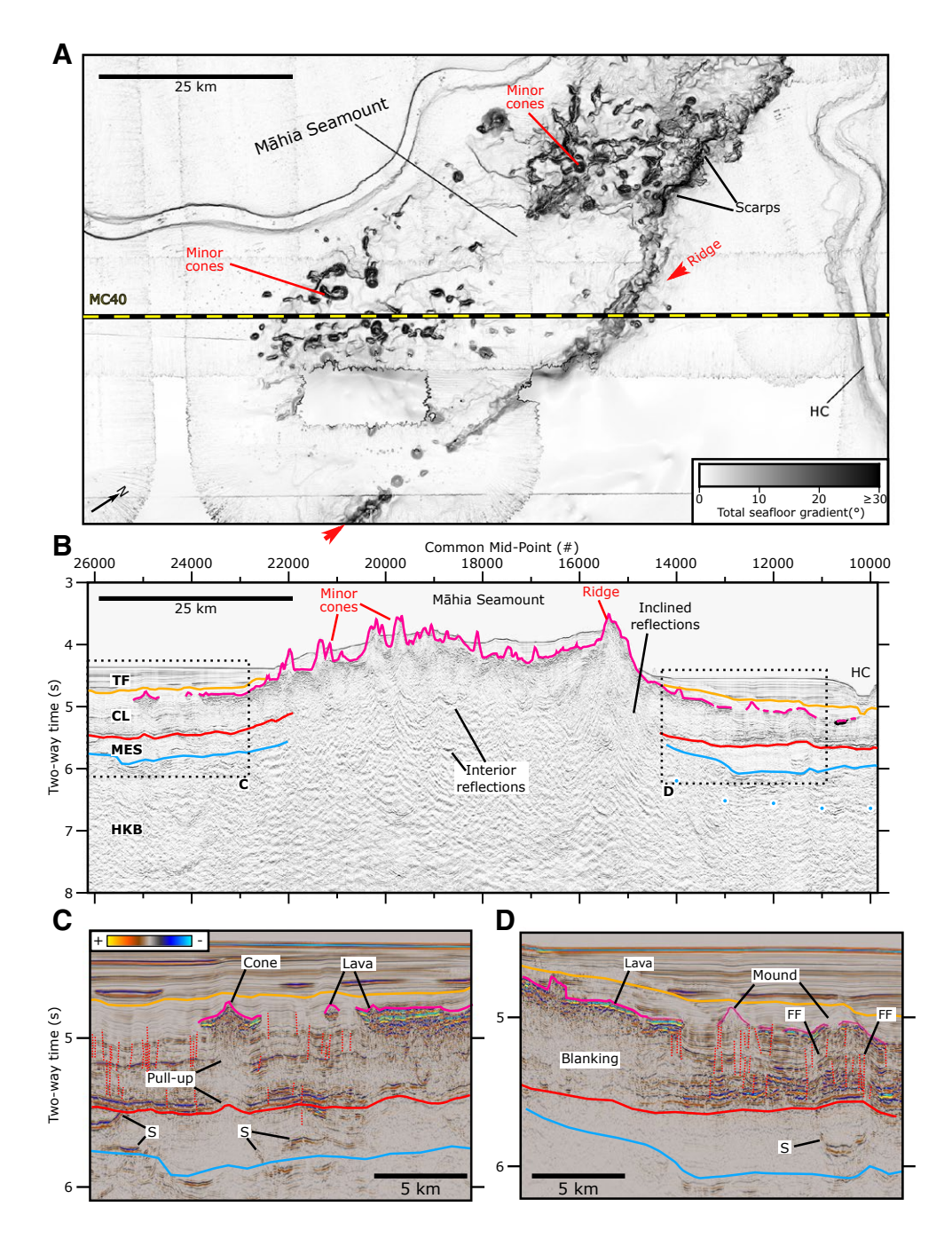


Figure 7. (A) Line-adjacent bathymetric gradient map. (B) Pre-stack time-migrated image of Māhia Seamount from Seismogenesis at Hikurangi Integrated Research Experiment Line 4/MC40 (Fig. 5). (C) Enlarged view of Māhia Seamount's southern flank. (D) Enlarged view of Māhia Seamount's northern flank. Stratigraphic horizons include the top of late-stage volcanics (magenta line), the Reflector 5b unconformity (yellow line), which separates trench-fill hemipelagic sediments (TF) from calcareous pelagic sediments (CL), the horizon that separates Sequence Y from Unit MES (Mesozoic sediments; red line), the top of Unit HKB (Hikurangi Plateau basement; blue line), and Horizon B (blue dots). FF-forced fold; HC-Hikurangi Channel; S-volcanic sill. Faults are marked by thin, subvertical dashed red lines. Vertical exaggeration is 6.5 at 2.5 km/s.

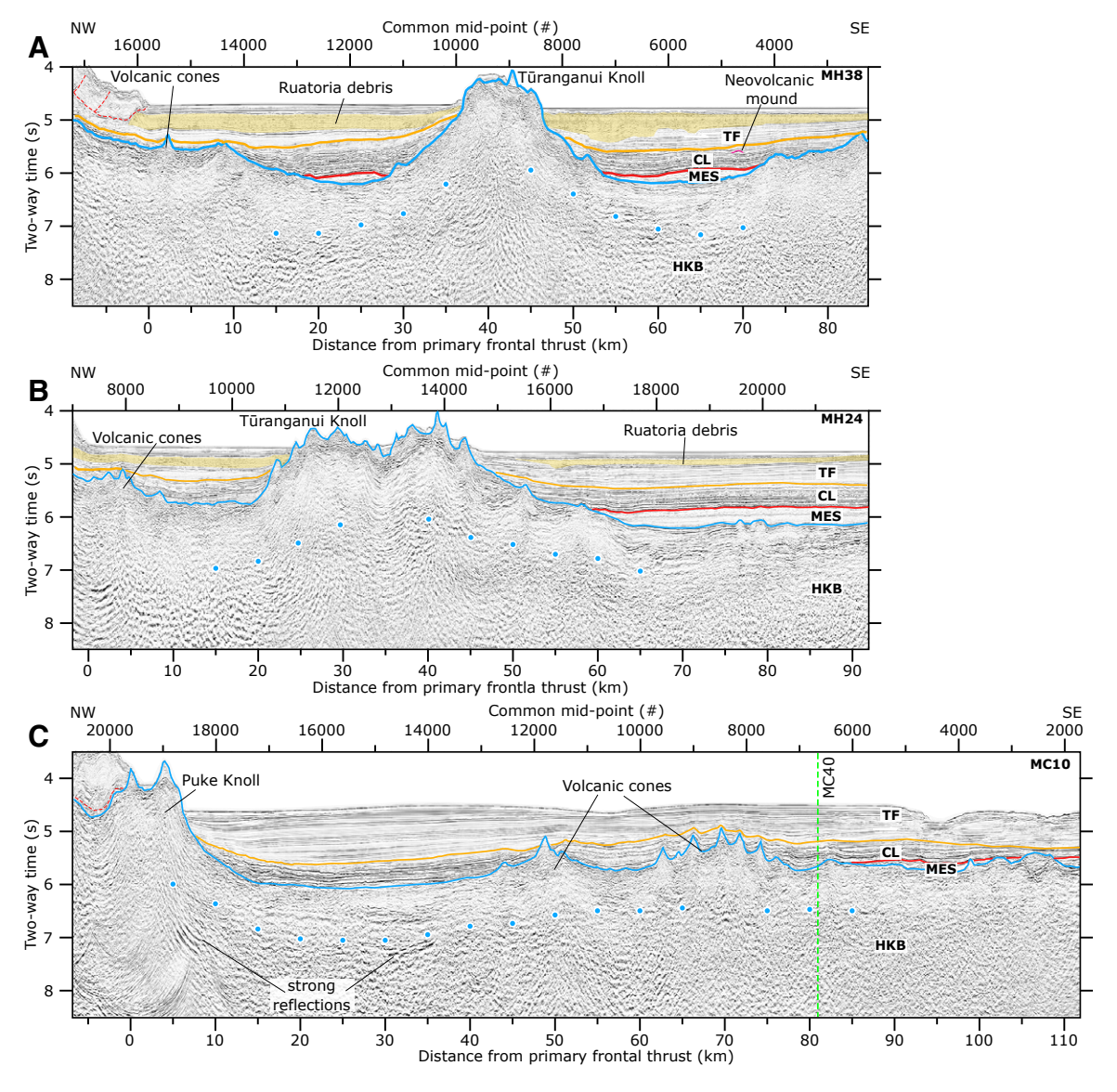


Figure 8. Pre-stack time-migrated images of seismic profiles (A) MH38, (B) MH24, and (C) Seismogenesis at Hikurangi Integrated Research Experiment Line 1b/MC10. Stratigraphic horizons follow the same conventions as in Figures 4 and 5. Stratigraphic horizons include the top of late-stage volcanics (magenta line), the Reflector 5b unconformity (yellow line), which separates trench-fill hemipelagic sediments (TF) from calcareous pelagic sediments (CL), the horizon that separates Sequence Y from Unit MES (Mesozoic sediments; red line), the top of Unit HKB (Hikurangi Plateau basement; blue line), and Horizon B (blue dots). Thrust faults in the outer wedge of the Hikurangi prism are shown as thin, dashed red lines. The Ruatoria debris avalanche deposit is shaded yellow. Vertical exaggeration is 5 at 2.5 km/s.

Puke Knoll. These banded reflections continue beneath the large seamounts, where they weaken. We suspect that these basement reflections may be related to a pre-seamount volcanic basement.

4.3. North-Central Profiles Offshore Hawke Bay

Seismic profiles MC55 and MC53 trend perpendicular to the margin (Fig. 9). The northernmost profile, MC55 (Fig. 9A), traverses the southern crest of Māhia Seamount, whereas MC53 (Fig. 9B) is located several kilometers south of the seamount. As observed in SHIRE Line 4/MC40, bright reflections

with chaotic interior fabric emanate from the top of Māhia Seamount, cover the lower strata of Unit CL, and are onlapped by the trench-wedge facies. These reflections are consistent with Pliocene volcanism (Timm et al., 2010). Contemporaneous neovolcanics are also observed to the south in profile MC53 (Figs. 9B, 10A, and 10B), and ~40 km to the west, near the Hikurangi margin deformation front. Reflections beneath the neovolcanic units have weaker amplitudes, which suggests scattering within the volcanic material and/or physical disruption of the underlying strata by dikes (Fig. 10). We interpret bright, discontinuous reflectors within units CL and MES as magmatic sills (Fig. 10). Normal faults cut units CL and TF, often along the margins of neovolcanics (Figs. 9 and 10), which indicates Quaternary deformation. Some

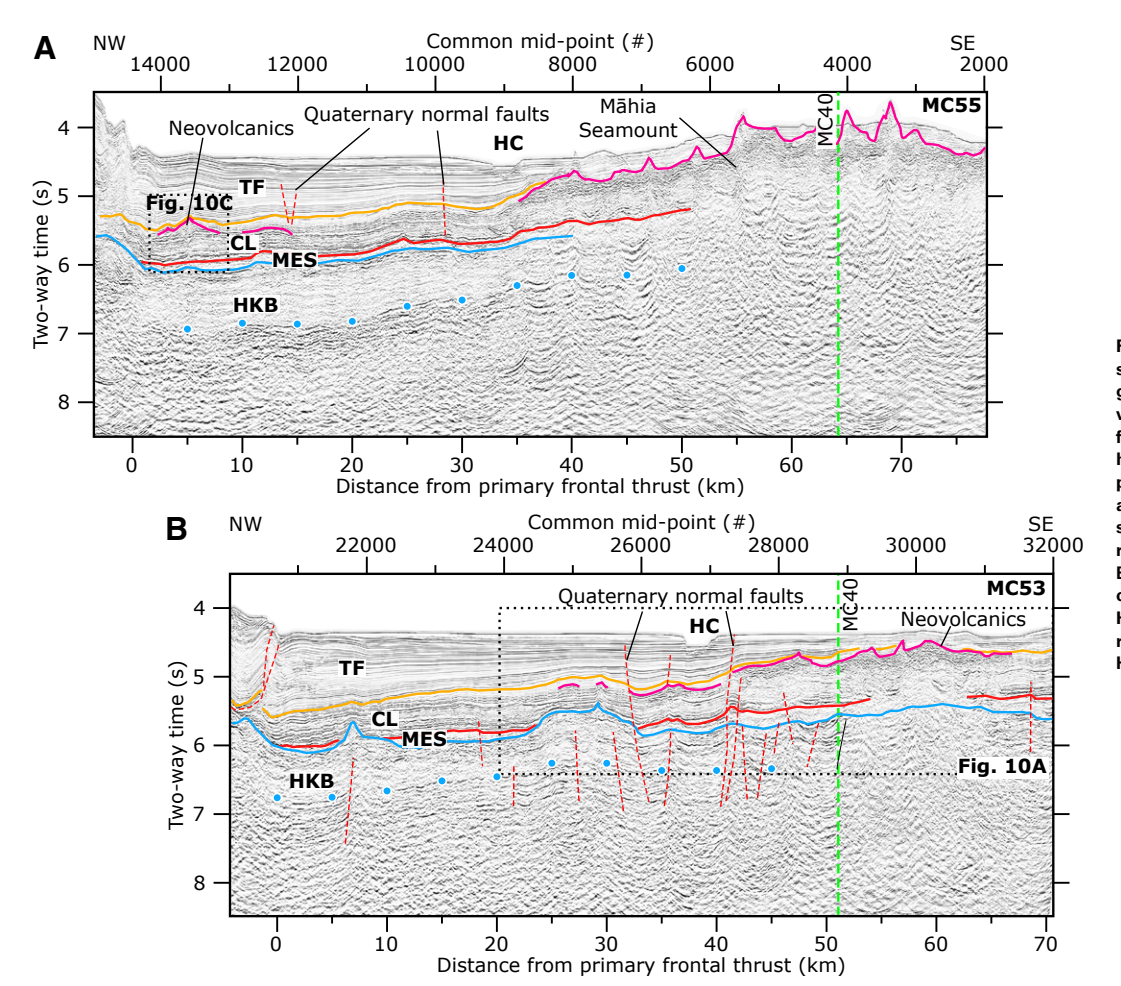


Figure 9. Pre-stack time-migrated images of seismic profiles (A) MC55 and (B) MC53. Stratigraphic horizons include the top of late-stage volcanics (magenta line), the Reflector 5b unconformity (yellow line), which separates trench-fill hemipelagic sediments (TF) from calcareous pelagic sediments (CL), the horizon that separates Sequence Y from Unit MES (Mesozoic sediments; red line), the top of Unit HKB (Hikurangi Plateau basement; blue line), and Horizon B (blue dots). Thrust faults in the outer wedge of the Hikurangi prism and normal faults of the Hikurangi Plateau are shown as thin, dashed red lines. Vertical exaggeration is 5 at 2.5 km/s. HC—Hikurangi Channel.

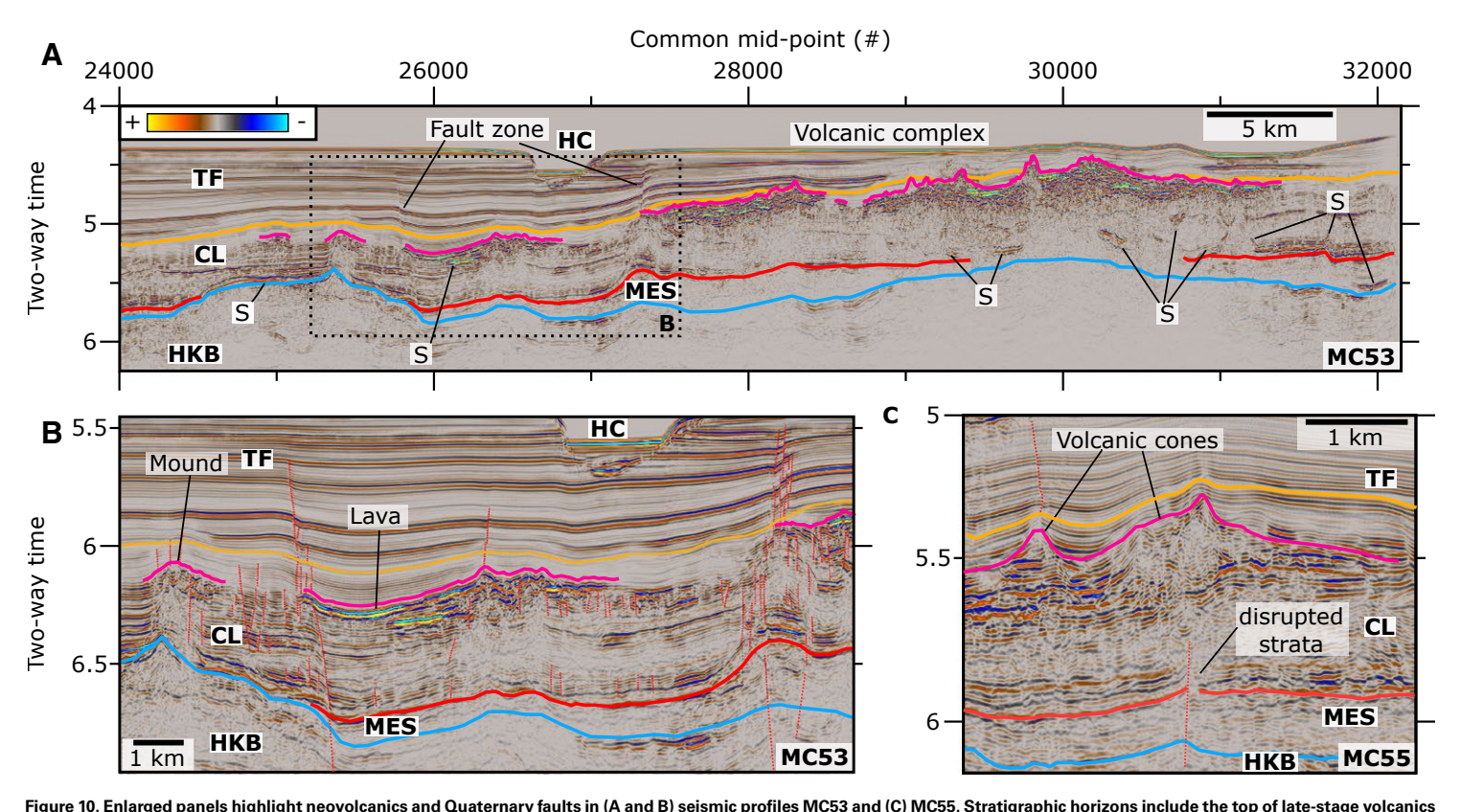


Figure 10. Enlarged panels nightight neovoicanics and Quaternary faults in (A and B) seismic profiles MUC33 and (C) MUC35. Stratigraphic norizons include the top of late-stage voicanics (magenta line), the Reflector 5b unconformity (yellow line), which separates trench-fill hemipelagic sediments (TF) from calcareous pelagic sediments (CL), the horizon that separates Sequence Y from Unit MES (Mesozoic sediments; red line), the top of Unit HKB (Hikurangi Plateau basement; blue line), and Horizon B (blue dots). S—volcanic sill; faults are marked by thin, subvertical dashed red lines. Vertical exaggeration at 2.5 km/s is 3.8 for parts A and B, and 2.4 for part C. HC—Hikurangi Channel.

faults appear to extend into Unit HKB. We suggest that the Quaternary faults could be related to differences in compaction of the volcanic and nonvolcanic sediments, thermal subsidence, inherited crustal weakness near neovolcanic activity, and/or plate bending.

As in profile MC40 (Fig. 5), the top of Unit HKB is often obscured beneath the neovolcanics on and adjacent to Māhia Seamount. This horizon has a gentle apparent dip to the northwest in profile MC55 (Fig. 9A) and is marked by ~0.25-s-high volcanic edifices in profile MC53 (Fig. 9B). The upper ~0.5–1 s of Unit HKB is weakly reflective. However, a clear, strong band of northwest-dipping reflections is observed at ~6–7 s in both profiles—a time that corresponds with bands of intra-basement reflections in the northern profiles (Fig. 8). We suggest that the top of this band of reflections is Horizon B and

likely represents the basement surface upon which seamounts were erupted. We infer volcaniclastic sediments to be more likely than lava flows in the upper \sim 0.5–1 s of Unit HKB here due to the general lack of strong reflectivity.

4.4. Central Profiles Offshore Porangahau

Seismic profiles MC50, MC58, and MC48 are located offshore the central Hikurangi margin near Pōrangahau, and are oriented perpendicular to the margin (Fig. 11). Here, the outer Hikurangi forearc transitions from a narrow, steep accretionary prism in the north to a wide, low-taper accretionary prism with abundant proto-thrusts up to 30 km seaward of the primary frontal thrust

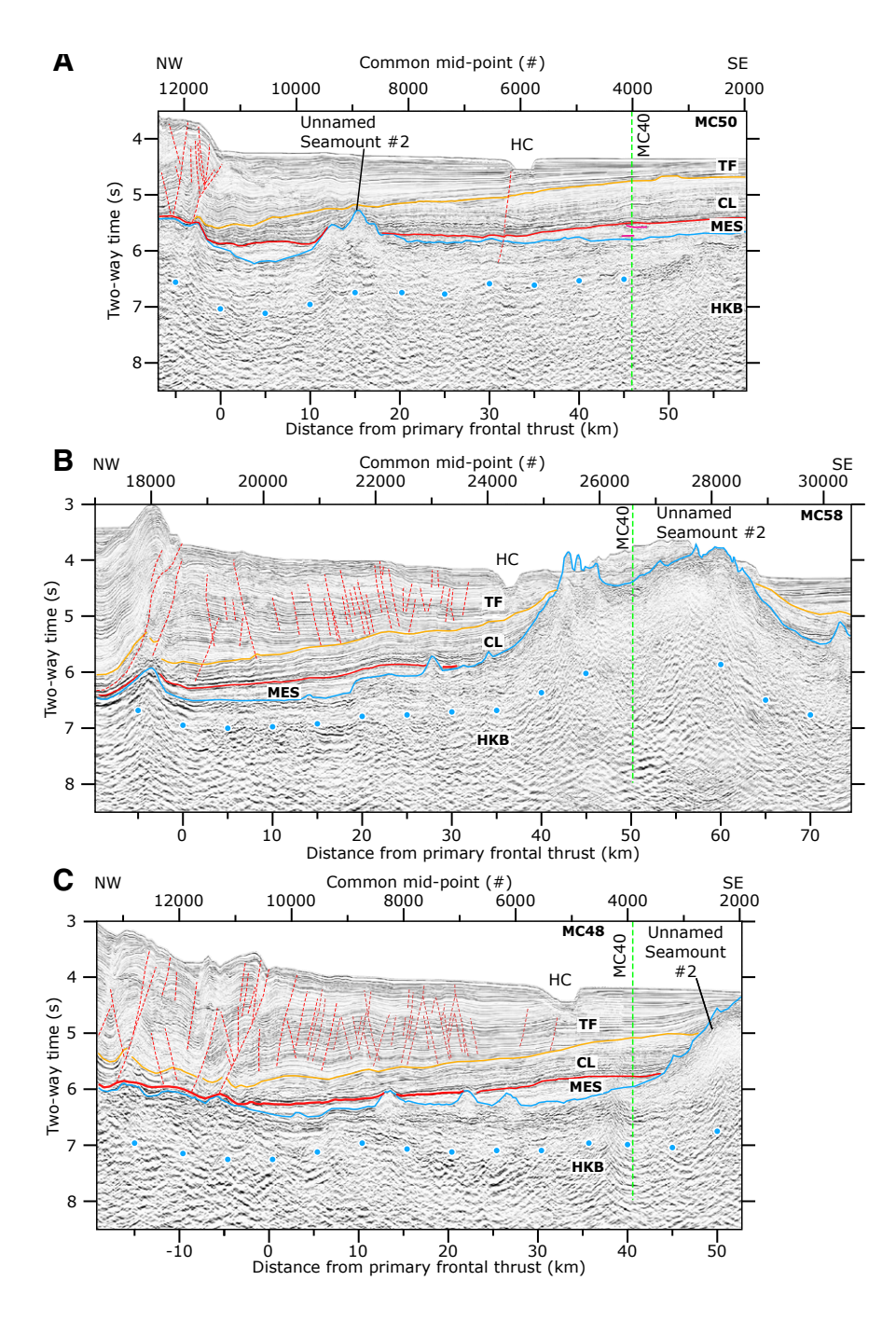


Figure 11. Pre-stack time-migrated images of seismic profiles (A) MC50, (B) MC58, and (C) MC48. Stratigraphic horizons include the top of late-stage volcanics (magenta line), the Reflector 5b unconformity (yellow line), which separates trench-fill hemipelagic sediments (TF) from calcareous pelagic sediments (CL), the horizon that separates Sequence Y from Unit MES (Mesozoic sediments; red line), the top of Unit HKB (Hikurangi Plateau basement; blue line), and Horizon B (blue dots). Faults are shown as thin, dashed red lines. Vertical exaggeration is 5 at 2.5 km/s. HC-Hikurangi Channel.

(Barnes et al., 2018; Figs. 1B and 11). Subhorizontal bright reflections with <5 km horizontal extents are observed in Unit MES in the northernmost profile (MC50; Fig. 11A), which we interpret as neovolcanic sills from the region surrounding Māhia Seamount. No other evidence of Cenozoic volcanism is observed in the southern profiles (MC58 and MC48; Figs. 11B and 11C). A basement-offsetting Quaternary normal fault is located beneath the western flank of the Hikurangi Channel in profile MC50 (Fig. 11A), but Quaternary deformation in the other profiles is only associated with subduction-induced thrust faults (Figs. 11B and 11C).

The upper Unit HKB surface in all three profiles contains segments of Unnamed Seamount #2. In profile MC50, Unnamed Seamount #2 is an ~0.75-s-high edifice with two peaks that lies 15 km from the deformation front (Fig. 11A). In profile MC58, ~35 km to the south, Unnamed Seamount #2 is a >50-km-wide ridge that rises >2 s above the surrounding basement topography (Fig. 11B). An ~15-km-long segment of its edifice is imaged at the eastern end of profile MC48 (Fig. 11C). Minor, 0.25-s-high volcanic cones are observed west of the Hikurangi Channel on profiles MC58 and MC48 (Figs. 11B and 11C). Reflections inside the upper ~1 s of Unnamed Seamount #2 include (1) strong, chaotic reflections at the center of the edifice on MC50 (Fig. 11A) and (2) steeply inclined reflections that dip away from the seamount's peak in profiles MC58 and MC48, where they are clearly constructed on the upper reflections of Unit HKB (Figs. 11B and 11C). These inclined reflections within Unnamed Seamount #2 continue into ~20-30-km-wide zones of relatively flat-lying and chaotic reflections that we interpret as lavas and volcaniclastic debris fans. The deep, layered reflections associated with Horizon B of the north-central Hikurangi margin (Fig. 9) are not clearly observed here. However, we note a horizon of increased higher reflection amplitude ~0.5-1.25 s below the top of Unit HKB in all three profiles, which we interpret as Horizon B (Fig. 11). This horizon is continuous with strong inclined reflections beneath Unnamed Seamount #2 at ~6-7 s that are consistent with our interpretation of the seamount interior reflections in other profiles (Figs. 5, 6, and 8).

4.5 South Profiles at Pegasus Basin

The southernmost profiles presented here, MC42, MC44, and PEG 09-08m1000, are located in the Pegasus Basin, offshore the Wairarapa coast (Fig. 12). The two southernmost SHIRE profiles (MC42 and MC44) are oriented perpendicular to the margin, whereas PEG 09-08m1000 trends northeast-southwest, approximately parallel to the deformation front. Trench-fill sediments in the Pegasus Basin increase southward to thicknesses of up to 6 km (Plaza-Faverola et al., 2012; Bland et al., 2015; Crutchley et al., 2020), and Unit MES thickens substantially into the extinct accretionary wedge of the Gondwana margin at the Chatham Rise (Fig. 12). We find no neovolcanic features in the Pegasus Basin. Quaternary faults in the sedimentary cover with significant throw are associated with the Hikurangi margin accretionary wedge system (Figs. 12A and 12B).

The upper Unit HKB surface shows the waning contribution of Late Cretaceous seamount volcanism from the northeast into the southwestern Pegasus Basin (Fig. 12). In profiles MC42 and MC44, the upper Unit HKB surface has an apparent gentle dip toward the Hikurangi margin forearc (Figs. 12A and 12B). In PEG 09-08m1000, this surface drops ~1.2 s from the northeast to the southwest under the inactive East Gondwana accretionary wedge (Fig. 12C). Small (<5-km-wide) volcanic cones are imaged at ~30 km in MC42 (Fig. 12A) and ~0–25 km in PEG 09-08m1000 (Fig. 12C); otherwise, the surface of Unit HKB is smooth and not influenced by distributed volcanism. The southeastern edge of profiles MC42 and MC44 (Figs. 12A and 12B) includes the flank of Unnamed Seamount #1. The upper ~0.25–1 km of the seamount's flank is marked by gently dipping wedges of reflections that we interpret as volcaniclastic debris or lava flows.

Below its surface, Unit HKB contains substantial reflectivity that may predate seamount volcanism. A strong, laterally continuous reflector in profile MC42 beneath Unnamed Seamount #1 shallows to where it is close to the surface of Unit HKB at ~10-40 km from the deformation front (Fig. 12A). This horizon agrees with the position of Horizon B in profile MC40 (Fig. 5), and we interpret it as the below-seamount basement interface. Such a strong Horizon B is not observed in profiles MC44 or PEG 09-08m1000; however, we do interpret a less prominent horizon within Unit HKB to represent the same interface (Figs. 12B and 12C). Our interpretation suggests that Horizon B outcrops at the Unit HKB upper surface near 40 km in profile PEG 09-08m1000 and is not identified beneath the Chatham Rise (Fig. 12C). We observe ~0.5-2-s-thick wedges of strong dipping reflections beneath Unit HKB's upper surface and Horizon B in all three profiles. In MC42 and MC44, these reflective wedges have an apparent dip to the northwest toward the Hikurangi margin forearc (Figs. 12A and 12B). In PEG 09-08m1000, they dip both southwest under the East Gondwana wedge of the Chatham Rise (distance 70-110 km) and northeast (distance 20-60 km; Fig. 12C). We interpret these wedges of dipping reflectors as lava flows, due to their similarity to seaward-dipping reflectors from lava flows on volcanic passive margins (Planke et al., 2000) and convex upward reflectors from lava flows on the Shatsky Rise (Sager et al., 2013). Small offsets in these dipping basement reflectors are interpreted as distributed normal faults that are no longer active.

4.6. Mapped Basement Topography

We mapped the top of the horizon of Unit HKB and neovolcanic reflectors across the margin, including legacy seismic surveys and all SHIRE seismic profiles across the Hikurangi Plateau (Fig. 13; see Table S1 for legacy survey information). Neovolcanics are widely observed in the north-central portion of the margin surrounding Māhia Seamount and less so around Tūranganui Knoll (Fig. 13). Lower volumes of neovolcanics may exist throughout the margin, however; our 2-D lines with nominal spacing of ~10–40 km are capable of imaging neovolcanic features of this scale.

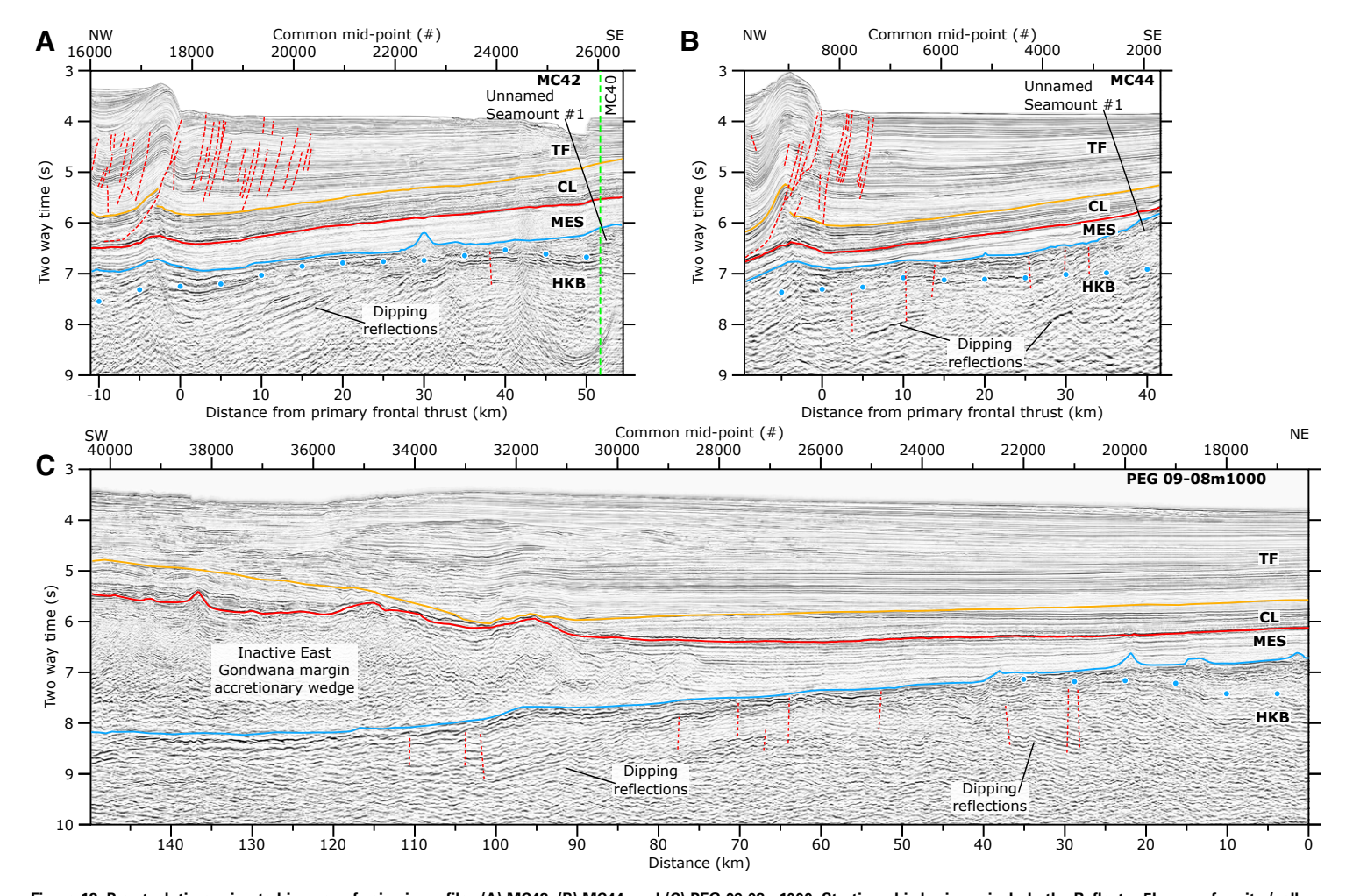


Figure 12. Pre-stack time-migrated images of seismic profiles (A) MC42, (B) MC44, and (C) PEG 09-08m1000. Stratigraphic horizons include the Reflector 5b unconformity (yellow line), which separates trench-fill hemipelagic sediments (TF) from calcareous pelagic sediments (CL), the horizon that separates Sequence Y from Unit MES (Mesozoic sediments; red line), the top of Unit HKB (Hikurangi Plateau basement; blue line), and Horizon B (blue dots). Faults are shown as thin, dashed red lines. Vertical exaggeration is 5 at 2.5 km/s.

From the upper horizon of Unit HKB, we interpret at least seven major seamounts along the margin, including Tūranganui Knoll, Puke Knoll, Te Kuria-Paoa Seamount, Māhia Seamount, Unnamed Seamount #1, Bennett Knoll, and Unnamed Seamount #2 (Fig. 13). The largest of these seamounts are up to 100 km long in their greatest dimension. All seamounts north of Bennett Knoll have a clear north–south or northwest–southeast alignment. Poor data

coverage to the south and east of Unnamed Seamount #1 prevents us from determining its geometry. Türanganui Knoll and Te Kuri-a-Paoa Seamount may be interpreted as a single volcanic structure due to their proximity and consistent orientation. The regional basement topography along the Hikurangi margin deformation front gradually descends from ~4 km b.s.l. offshore Gisborne to ~12 km b.s.l. in the western Pegasus Basin.

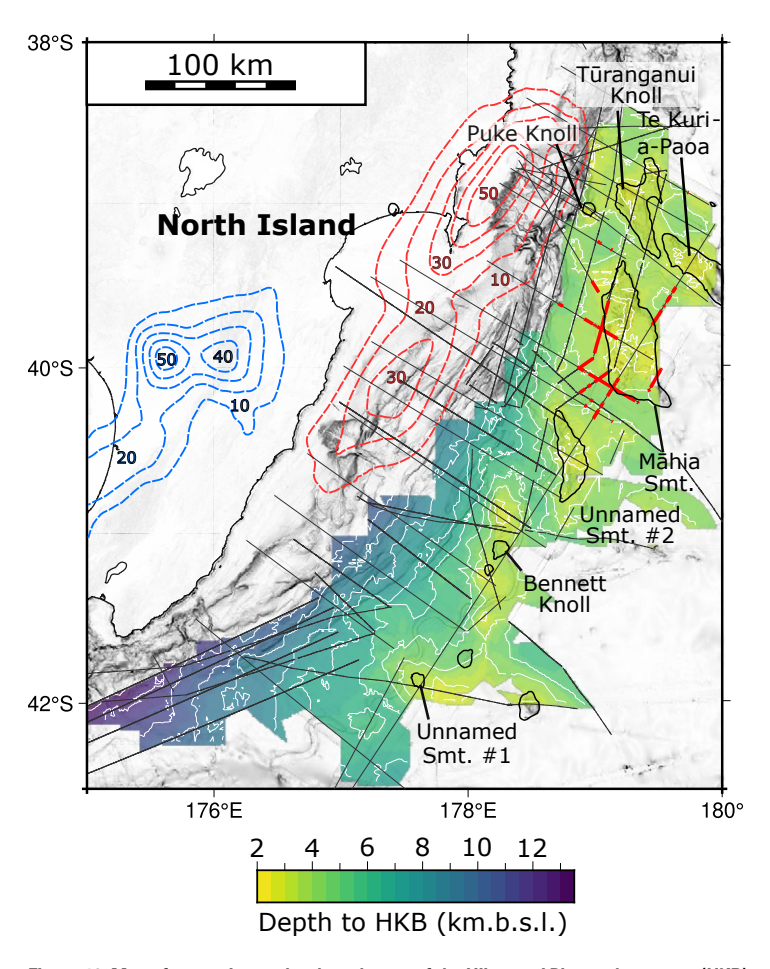


Figure 13. Map of approximate depth to the top of the Hikurangi Plateau basement (HKB) unit along the Hikurangi margin, North Island of New Zealand. Neovolcanics observed on 2-D seismic profiles are plotted as thick red lines. Cumulative slow slip (in centimeters) between 2002 CE and 2014 CE is plotted in red (shallow; i.e., < 20 km) and blue (deep; i.e., >20 km) contours (Wallace, 2020).

5. DISCUSSION

5.1. Basement Structure and Geologic Evolution of the Hikurangi Plateau

Large igneous provinces and oceanic plateaus are sites of voluminous supply of magma from the deep Earth to the upper mantle and crust in a relatively short time (e.g., Coffin and Eldholm, 1994; Self et al., 2013). High-magmatic flux can result in crustal intrusion, which thickens the crust from within, and massive eruptions that thicken the basaltic upper crust. Thus, oceanic plateaus have crust, measured from the top of the basaltic basement to the Moho discontinuity, which is ~1.5-5 times thicker (Coffin and Eldholm, 1994) than normal oceanic crust (~6 km; Van Avendonk et al., 2017; Chen, 1992; Christeson et al., 2019; White et al., 1992). Although not well studied, some plateaus, including Manihiki (Hochmuth et al., 2019) and Ontong Java (Tonegawa et al., 2019), have regional variations in their crustal thickness that could be related to rifting or heterogeneous supply of magma. The relative contribution of intrusion and volcanic eruptions to crustal thickening is not well known. Large seamounts can locally increase the thickness of basaltic oceanic crust by up to 3 km without coincident underplating (Bassett et al., 2023). Seismic profiling across the Hikurangi Plateau demonstrates that it is thickest at its southern margin (10-16 km) near the Chatham Rise (Mochizuki et al., 2019; Herath et al., 2020; Riefstahl et al., 2020a; Bassett et al., 2023) and thins (7-10 km; Scherwath et al., 2010; Gase et al., 2021; Bassett et al., 2023) toward its northeastern boundary, where rifting occurred between the Hikurangi and Manihiki plateaus (Taylor, 2006).

Less is known about the structure and lithological composition of the Early Cretaceous Hikurangi Plateau basement and whether it was modified by plateau rifting. This is complicated by the volume and prevalence of seamount volcanism that is believed to be of Late Cretaceous age (Hoernle et al., 2010). At other oceanic plateaus (e.g., Manihiki Plateau, Ontong Java Plateau, and Shatsky Rise), drilling and seismic imaging show that LIP eruptions produce massive lava sheet flows (Jackson et al., 1976; Tarduno et al., 1991; Koppers et al., 2010; Sager et al., 2013), which indicate high-eruption rates and are analogous to continental flood basalts (Self et al., 2013). Sheet flows can be interbedded with or covered by pillow lavas and volcaniclastic materials. When viewed seismically, these volcanic flows appear as flat-lying packages (Inoue et al., 2008; Bangs et al., 2015) or inclined wedges (Parsiegla et al., 2008; Sager et al., 2013; Zhang et al., 2015; Pietsch and Uenzelmann-Neben, 2015) of continuous reflections beneath the top of the basement, similar to seaward-dipping reflectors at volcanic rifted margins (e.g., Planke et al., 2000). We believe that the dipping reflections observed in the Pegasus Basin are massive sheet flows from eruptions (Fig. 12), possibly from the Early Cretaceous Hikurangi Plateau formation. The dipping reflectors can also be viewed in other seismic reflection profiles within the Pegasus Basin presented elsewhere (Bland et al., 2015; McArthur and McCaffrey, 2019), which indicates that they are a common uppercrustal structure within this region. Similar inclined reflections are documented on the Manihiki Plateau (Pietsch and Uenzelmann-Neben, 2015), which lacks Late Cretaceous seamount volcanism (Hoernle et al., 2010; Timm et al., 2011). The possibility that the dipping reflectors on the Hikurangi Plateau are a part of the Early Cretaceous basement is further supported by (1) the lack of post-LIP formation volcanism in the form of large seamounts and thick volcaniclastic deposits in the Pegasus Basin; (2) the fact that the dipping massive sheet flows extend beneath the extinct East Gondwana margin accretionary prism of the Chatham Rise (Fig. 12C), where convergence ceased in the Late Cretaceous

(Davy et al., 2008; Davy, 2014; Mortimer et al., 2020; van de Lagemaat et al., 2023), approximately the same period when large seamounts erupted across the Hikurangi Plateau (Hoernle et al., 2010); and (3) the Pegasus Basin is far (~400–600 km) from the locus of Late Cretaceous plateau rifting and crustal thinning (Bassett et al., 2023).

Northeast of the Pegasus Basin, we propose that the Early Cretaceous Hikurangi Plateau basement is locally obscured by deformation from rifting and Late Cretaceous seamount volcanism. The stronger Horizon B imaged along the north-central Hikurangi margin (Fig. 9) and the diffuse increase in intra-basement reflectivity on other profiles (Figs. 5, 8, and 11) are ideal candidates for the northern continuation of the top of the Early Cretaceous basement. We demonstrate that many of the Hikurangi Plateau seamounts contain strong reflections that are continuous with the inferred Horizon B across the Hikurangi Plateau. This horizon could be obscured in some regions by scattering from overlying volcanic deposits or disrupted by magmatic intrusion and rifting.

Gravity data and wide-angle profiling show that crustal thinning from plateau rifting occurred at the northern and north-central Hikurangi Plateau (Bassett et al., 2023); however, the effect of this process on the Hikurangi Plateau's upper crustal structure is unclear. Although normal faults would be expected to accompany crustal thinning, large-offset Cretaceous-age normal faults are not clearly observed in our data. Large-offset normal faults are reported in other studies near the Rapuhia Scarp and the remainder of the Hikurangi Plateau's northern rifted boundary (Davy and Collot, 2000; Davy et al., 2008). The lack of evidence of Cretaceous deformation in our study area could also be due to geologic overprinting and seismic scattering by the Late Cretaceous seamount volcanism or the tendency of our seismic profiles to be oriented oblique to the north-south trend of Cretaceous subduction at the Chatham Rise and rifting to the north. Large seamounts between the central and northern Hikurangi Plateau are elongated north-south or northwest-southeast (Fig. 13). This consistent seamount orientation persists farther north to the Hikurangi Plateau rifted margin (Davy et al., 2008; Hoernle et al., 2010), which indicates that the seamounts' magma supply was influenced by anisotropic crustal permeability, perhaps caused by rift-related faults or a prevailing minimum principal stress that was oriented north-south to northwest-southeast.

Volcaniclastic deposits are prevalent above Horizon B northeast of the Pegasus Basin, often reaching thicknesses of 0.5–1 s at the flanks of large seamounts. Our images show that these volcaniclastic deposits are widespread throughout the central and northern Hikurangi margin and gradually thin to distances of up to 30 km from the seamounts' peaks, which implies that they are partially sourced from the large seamounts as volcaniclastic debris and lava flows (Barnes et al., 2020). Scattered minor volcanic cones within Unit HKB also suggest that smaller, distributed volcanic eruptions could be the source of some of these upper volcanic deposits.

Horizon B is a candidate for the top of basaltic basement with properties that are similar to upper normal oceanic crust, and overlying volcaniclastic deposits may have much more variable characteristics. Wide-angle seismic tomography studies find that the volcaniclastic deposits above Horizon B can

have P-wave velocities of <5 km/s to depths 2-3 km below the top of Unit HKB (Scherwath et al., 2010; Arai et al., 2020; Gase et al., 2021; Bassett et al., 2023). Full-waveform inversion, well-logging, and stacking velocities further demonstrate that the upper ~1.5 km of Unit HKB can have very low-P-wave velocities (1.8-4 km/s; Davy et al., 2008; Barker et al., 2018; Gray et al., 2019; Barnes et al., 2020; Bangs et al., 2023; Gase et al., 2023) compared to the top of normal Cretaceous-age basaltic ocean crust (>5.5 km/s; Christeson et al., 2019). Small volcanic cones and the adjacent volcaniclastic basins have little difference in their seismic velocities (Gase et al., 2023). In contrast, the seismic velocities of the interiors of large seamounts are ~1 km/s faster than those of the surrounding volcanic upper crust (Gase et al., 2021; Bassett et al., 2023), which could be the result of seismically fast magmatic intrusions or different eruption mechanisms on large seamounts. The flat, quyot-style upper surfaces of some of the largest seamounts of the Hikurangi Plateau imply that water depths were at least ~2.5 km shallower in the Late Cretaceous (Hoernle et al., 2004; Allen et al., 2022). Eruption styles (e.g., explosive versus effusive) can be strongly influenced by water depth (White et al., 2015). Possibly, some eruptions on the large seamounts occurred subaerially, whereas eruptions on smaller seamounts occurred in deep- or shallow-water conditions. Large seamounts may contain seismic velocity heterogeneities that result in adjacent zones of faster and slower seismic velocities (Arai et al., 2020; Bassett et al., 2023). This observation was independently confirmed by marine electromagnetic methods that found electrically conductive volcanic deposits on the flanks of large seamounts and heterogeneous electrical conductivity within the large seamounts that may be related to faulting, porosity anomalies, and rock alteration (Chesley et al., 2021). Determining whether the properties of these upper volcanic deposits vary systematically along the Hikurangi Plateau or with distance from large seamounts will require further investigation.

5.2. Cenozoic Volcanism and Deformation

Our newly presented evidence of Cenozoic volcanism provides new constraints on the distribution of neovolcanic activity in the western region of the Hikurangi Plateau. Late Cenozoic volcanic activity is not limited to the Hikurangi Plateau, and in fact is widespread throughout the continental crust of Zealandia (Timm et al., 2010). What supplied magma to the Hikurangi Plateau after >60 m.y. of volcanic dormancy is not obvious, and rejuvenation of Late Cretaceous magma sources is improbable.

Distributed intraplate volcanoes near oceanic trenches, so-called "petit-spot volcanoes," are observed in subduction zones with high-degrees of outer-rise flexure, which leads to the hypothesis that flexure and faulting release melt from the mantle (Hirano et al., 2001, 2006, 2008; Valentine and Hirano, 2010). Subsequent geochemical analyses of petit-spot volcanoes from the Northwest Pacific, Samoa, and the Christmas Islands reveal alkali basalts with an enriched mantle source (EM1; Hoernle et al., 2011; Reinhard et al., 2019; Hirano and Machida, 2022). The Japan Trench petit-spot volcanoes have spatially

and temporally distinct trace-element compositions that cannot be explained by crystal fractionation, which indicates that low-degree partial melts can percolate through the lithosphere without significant storage (Machida et al., 2015). Yang and Faccenda (2020) proposed that in the Northwest Pacific, where the Pacific Plate slab has stagnated in the mantle transition zone, seismic low-velocity zones above the 440–660 km depth mantle transition zone indicate hydrous melting of the upper mantle that could lead to melt ponding near the lithosphere–asthenosphere boundary and serve as the source of the petit-spot volcanoes.

Petit spot volcanism can also modify the seismic structure and properties of the shallow basement and sedimentary stratigraphy. Ohira et al. (2018) reported reduced upper-crustal P-wave velocities, opaque basement reflections, and weakened Moho reflections under petit-spot volcanoes in the Japan trench. These late-stage eruptions can disrupt and metamorphose sediments on subducting plates, and both are factors that may influence material properties and structure along the megathrust once petit-spot volcanic provinces subduct (Fujie et al., 2020).

The neovolcanics observed near Māhia Seamount are possibly petit-spot volcanoes. At the Hikurangi margin, lithospheric flexure is reduced compared to other margins with petit-spot volcanoes, due to the thickened crust of the Hikurangi Plateau (Bassett et al., 2023). However, free-air gravity anomalies along the Hikurangi margin data still detect an ~300-km-wide gravity high outboard of the Hikurangi Trough that is continuous with the outer rise of the Kermadec Trench (Bassett et al., 2023). Assuming constant flexure and plate velocities (~5 cm/yr) over time, Māhia Seamount was in this flexural bulge 3.3 m.y. ago, when the neovolcanics erupted. We observe few recently active normal faults along the margin except for the region of neovolcanic activity, which implies a link between intraplate deformation and volcanism. Timm et al. (2011) showed that Māhia Seamount's Pliocene lavas are basanites (i.e., low-silica alkali basalts) with a HIMU mantle source, which is consistent with other Cenozoic intraplate volcanism throughout Zealandia. Strong wide-angle seismic reflections beneath the Hikurangi Plateau Moho are attributed to partial melts within the lithosphereasthenosphere boundary at 80-100 km depth (Stern et al., 2015; Herath et al., 2022). Mather et al. (2020) proposed that widespread Cenozoic intraplate volcanism in Eastern Australia, Zealandia, and the South Fiji Basin (Mortimer et al., 2018) is caused by the displacement of volatiles from the mantle transition zone by the Pacific Plate slab. This mechanism is a possible source of neovolcanics on the Hikurangi Plateau. Alternative explanations could include partial melt channelization to the lithosphere-asthenosphere boundary from a mantle plume (Naif et al., 2023), but we consider this unlikely because no active hotspots are within 2000 km of the Hikurangi Plateau.

Active normal faults are often observed on many oceanic plateaus (Gün et al., 2024); however, whether subduction still induces substantial flexural deformation and faulting in thickened oceanic lithosphere is not well understood. In normal oceanic lithosphere, outer-rise flexural extension can alter the composition and porosity of the subducting plate through fracturing and chemical hydration reactions (Ranero et al., 2003; Van Avendonk et al., 2011;

Naif et al., 2015; Grevemeyer et al., 2018; Miller et al., 2021; Acquisto et al., 2022). Enhanced slab hydration in response to bend-faulting may influence rates of intermediate-depth, intra-slab seismicity (Shillington et al., 2015) and the chemical composition of volcanic arcs (Carr et al., 2003). However, the extent of contemporary normal faulting is strongly influenced by the orientation of preexisting abyssal hill fabric (Ranero et al., 2005), which is not known within the Hikurangi Plateau. Active flexural extension of the Hikurangi Plateau has been documented where the plateau's northern edge subducts along the southern Kermadec Trench, northeast of East Cape (Collot and Davy, 1998), presumably where the crust of the plateau is thinnest (Bassett et al., 2023). However, such deformation appears to be limited in the Hikurangi Trough, with evidence of recent normal faulting observed only near Māhia Seamount. Still, this does not rule out the possibility that the Hikurangi Plateau basement is heavily faulted nor that its lithosphere has been hydrated by other processes. Distributed normal faults are clear in the Pegasus Basin basement, where seismic energy is less likely to be scattered by thick volcaniclastic deposits or seamounts (Fig. 13), but these faults do not significantly deform the overlying strata. Intra-slab earthquakes with normal- and strike-slip mechanisms are prevalent across the Hikurangi forearc (Reyners et al., 2017; Todd et al., 2018; Yarce et al., 2019; Mochizuki et al., 2021), which indicates ongoing deformation within the subducting Hikurangi Plateau. Henrys et al. (2006) also infer, from coincident seismic reflection data and seismicity in Hawke Bay, that large normal faults formed or reactivated in the Hikurangi Plateau upon subduction. Wide-angle seismic profiling studies show variations in the Hikurangi Plateau's mantle P-wave velocities (7.9-9.0 km/s) that could be related to serpentinization, porosity, or changes in olivine mineral fabric (Mochizuki et al., 2019; Stern et al., 2020; Herath et al., 2020; Gase et al., 2021; Bassett et al., 2022). However, whether these seismic velocity variations are due to modern or ancient processes is unknown. Thus, slab-bending and hydration could be an important contemporary process within the Hikurangi forearc even if it were not pervasive before subduction.

5.3. Implications for Forearc Structure

Seamount collisions can have a strong influence on many structural factors in forearcs. At thinly sedimented margins, subducting seamounts can cause over-steepened forearcs and landslide scarps that can be readily identified from seafloor morphology (Ranero and von Huene, 2000; von Huene et al., 2004). Along the northern Hikurangi margin, where sediments are <1.5 km thick, large seamounts of the Hikurangi Plateau protrude through the sediment cover, and smaller-scale basement topography is buried. Here, the effects of large seamount collisions are widely documented as (1) a steeper prism taper (Fagereng, 2011); (2) large-scale collapse of the forearc (Lewis et al., 1998; Collot et al., 2001; Pedley et al., 2010); (3) radiating upper-plate deformation fabrics above seamounts (Barnes et al., 2010); (4) local variations in the volume and kinematics of frontally accreted sediments (Gase et al., 2021); and (5) spatial

variations in tectonic loading, consolidation, and stress state (Ellis et al., 2015; Sun et al., 2020). However, the effects of seamount subduction on forearc structure become more subtle when the thickness of sediments approaches the height of the seamounts. Numerical simulations show that when seamounts are buried by sediments and are higher than the décollement horizon (i.e., have relief exceeding the thickness of subducting sediments), deformation is partially accommodated by long-offset frontal thrust faults (Morgan and Bangs, 2017). Oversteepening is short-lived, and poorly consolidated sediments accrete in the seamount's wake (Morgan et al., 2022; Bangs et al., 2023).

Completely subducted seamounts are well observed along the north-central Hikurangi margin at Ritchie Banks (Nicol et al., 2007; Barker et al., 2009), Rock Garden (Barnes et al., 2010), and the northern Hikurangi margin offshore of Gisborne (Bell et al., 2010; Barker et al., 2018; Bangs et al., 2023). Former seamount subduction has also been inferred farther north at the Ruatoria reentrant (Lewis et al., 1998; Collot et al., 2001). Despite seamounts being observed along the entirety of SHIRE Line 4/MC40 outboard of the Hikurangi Trough, there is little evidence for major seamount subduction beneath the southern Hikurangi forearc (Barnes et al., 2010; Plaza-Faverola et al., 2012; Bland et al., 2015; Ghisetti et al., 2016; Crutchley et al., 2020; McArthur et al., 2020; Gase et al., 2022), other than the presently colliding Bennett Knoll (Davidson et al., 2020). Chow et al. (2022), however, suggest that a localized high-velocity feature within the inner central Hikurangi margin near Pōrangahau is a large seamount that subducted ~4 m.y. ago, potentially resulting in subsidence of the margin at Madden Canyon. Conversely, the effects of seamount subduction on forearc structure—such as oversteepening, long-offset thrusts, and collapses—have not yet been documented in the southern Hikurangi forearc.

Three-dimensional models of seamount collisions often assume that seamounts are conical structures with circular bases (Dominguez et al., 2000; Ruh et al., 2016). This assumption may be advantageous for isolating the effects of topography for a simple physical model but could fail to explain structures observed in natural systems. The size of the seamount compared to the thickness of incoming sediments and the seamount's geometry are important for understanding its impact on a subduction margin (Zeumann and Hampel, 2015). Large seamounts across the Hikurangi Plateau have consistent topographic relief (~2-3 km) above the regional basement. Because all incoming seamounts along the central and northern Hikurangi margin are elongated north-south- and northwest-southeast-trending ridges, conceptual models of seamount subduction at the Hikurangi margin should consider the possibility that subducted seamounts are long, linear ridges rather than single cones (Fig. 13). Due to their obliquity to the margin (~30° angle), these long volcanic ridges could influence ~50-100-km-wide segments of forearc diachronously. The height of the seamounts above the regional décollement should also be considered. At the northern Hikurangi margin, the megathrust forms within Unit HKB and Unit CL (Barnes et al., 2020; Gase et al., 2022, 2023). Along the central and southern Hikurangi margin, the décollement typically forms near the base of Unit CL above Sequence Y (Barnes et al., 2010). Across the Hikurangi margin, Unit MES thickens substantially, from ~0.5 km along the central Hikurangi margin to ~3 km in the southern Pegasus Basin (Plaza-Faverola et al., 2012); this thickness is sufficient to limit the impacts of minor basement roughness on the megathrust and would have limited the effective height of any formerly subducted larger seamounts if they had been present (Gase et al., 2022).

Seamounts and volcaniclastic rocks are documented in accretionary complexes elsewhere (Buchs et al., 2011; Clarke et al., 2018; Bonnet et al., 2020), and it is possible that some neovolcanics could have been frontally accreted into the Hikurangi forearc. Many of the Pliocene neovolcanic cones, sills, and lava flows observed in our data are located near the north-central Hikurangi margin deformation front above the proto décollement, which is in the base of Unit CL (Figs. 8A, 9, and 10). Whether such accretion would have any effect on forearc fault kinematics or properties is unknown. Accreted petit-spot volcanoes are documented onshore in the Santa Rosa accretionary complex of Costa Rica (Buchs et al., 2013). Petit-spot volcanics could form over the entire age of the subduction zone and be incorporated into the forearc wedge as they reach the deformation front. Our images of a reflective basement zone (Horizon B) within Unit HKB and the interior of large seamounts also raise the possibility that weak horizons could exist within the volcanic upper crust that allow for the scraping of volcanic material from the incoming plate (Clarke et al., 2018). Deep-sediment underplating is inferred beneath North Island of New Zealand (Scherwath et al., 2010; Bassett et al., 2010; Henrys et al., 2013), but the composition and origin of the underplated material are unknown. Stripping and underplating of upper-crustal volcaniclastics and basalt is a potential mechanism that has been replicated with numerical models (Ellis et al., 1999; Menant et al., 2020).

5.4 Implications for Slip Behavior

When fault rheology can be approximated as frictional, slip behavior is influenced by numerous factors, including effective normal stress (Leeman et al., 2016), slip rates (Ikari et al., 2013; Im et al., 2020), geometric conditions (Scholz, 1988; Scuderi et al., 2017), and rock frictional properties that depend on extrinsic conditions and lithology (Kurzawski et al., 2016; Rabinowitz et al., 2018; Boulton et al., 2019; Shreedharan et al., 2022, 2023). Because these factors can be at play on any fault simultaneously, it is difficult to determine their relative importance and how they may be affected by volcanic basement. Still, seamounts and rough volcanic basements are widely believed to influence slip behavior on subduction megathrusts (Wang and Bilek, 2014), although the exact reasons why are unclear and are, at times, in conflict (Mochizuki et al., 2008; Lee et al., 2023). Seamounts have been attributed to promoting slow slip and creeping behavior (Wang and Bilek, 2011; Barker et al., 2018; Shaddox and Schwartz, 2019) or influencing large earthquakes and fault locking (Cloos, 1992; Kodaira et al., 2000; Bell et al., 2014; Collot et al., 2017).

Effective normal stress of faults is generally correlated with stick-slip behavior in velocity-weakening materials (Scholz, 1998), and it depends on

overburden thickness and horizontal stresses, which are counteracted by elastic effects of trapped pore fluids (e.g., Saffer and Tobin, 2011). Recent numerical and geophysical studies suggest several ways that seamounts and volcaniclastic deposits along the northern and central Hikurangi margin could promote elevated pore-fluid pressures and heterogeneous stress conditions along the megathrust. Numerical simulations show that seamounts—approximated as large, rigid topographic asperities—can increase effective normal stress directly down-dip along the megathrust (Ruh et al., 2016; Martínez-Loriente et al., 2019; Sun et al., 2020), which is expected to promote stick-slip behavior. In contrast, the area immediately up-dip is shadowed from collisional stresses (Sun et al., 2020). Three-dimensional seismic imaging of subducted seamounts at the northern Hikurangi margin shows that these stress shadow zones can contain lenses of undrained sediments that can persist for long durations and appear in regions with well-documented shallow slow-slip events (Bangs et al., 2023). Seamounts and the adjacent volcaniclastic deposits on the Hikurangi Plateau can contain far more water than normal oceanic crust (Chesley et al., 2021; Gase et al., 2023) as a result of chemical alteration and greater porosity. If subducted seamounts or thick volcaniclastic deposits contain overpressured fluids that are hydraulically connected to the megathrust, they could limit stick-slip behavior. Changing stress conditions within the subducted Hikurangi Plateau, inferred from earthquake focal mechanisms, suggest that hydraulic connection between the Hikurangi Plateau and the megathrust is possible (Warren-Smith et al., 2019).

Investigators have long speculated from bathymetry that seamounts have less influence on the forearc structure and megathrust of the southern Hikurangi margin (Lewis et al., 1998; Wallace et al., 2009). Growing evidence from seismic imaging confirms that there is a greater influence of volcaniclastic lithologies and seamounts on the central and northern Hikurangi megathrust than on the southern megathrust (Collot et al., 2001; Barker et al., 2009; Barnes et al., 2010, 2020; Plaza-Faverola et al., 2016; Crutchley et al., 2020; Davidson et al., 2020; Gase et al., 2021, 2022, 2023; Bangs et al., 2023). This is supported by our observation of less prevalent volcaniclastic deposits and large seamounts in the Pegasus Basin (Figs. 12 and 13). Normal faults from Cretaceous rifting of the Hikurangi Plateau, concentrated in the northern and central Hikurangi Plateau, may have served as conduits for magmas that constructed the large seamounts and contributed to the thick volcaniclastic sequences observed. This could indicate an alongstrike change in the influence of volcanic lithologies on the Hikurangi margin's hydrogeology and stress state. However, this hypothesis cannot be verified without higher-resolution geophysical imaging (i.e., full-waveform inversion and 3-D reflection) and drilling across the Hikurangi Plateau.

In addition, other factors, such as lithology along the megathrust, could be important. Recovered volcaniclastic samples from the flank of Tūranganui Knoll are rich in smectite clays (Barnes et al., 2020; Underwood, 2021). Geomechanical tests demonstrate that these clay-rich volcaniclastic lithologies have slightly slip-weakening dynamic friction, do not heal efficiently, and are incapable of accumulating sufficient elastic strain for large earthquakes (Shreedharan et al., 2022, 2023). Such conditions could further promote shallow slow-slip

where the megathrust is composed of volcaniclastic lithologies (Barnes et al., 2020; Gase et al., 2022). In combination, these factors related to seamounts and the volcaniclastic upper crust of the Hikurangi Plateau could influence the northern Hikurangi margin's tendency for recurring slow slip and the southern Hikurangi margin's locked state (Wallace, 2020).

■ 6. CONCLUSIONS

In summary, we make several key points related to the volcanic history and structure of the Hikurangi Plateau near the trench of the Hikurangi subduction zone:

- (1) The Hikurangi Plateau formed through at least two major phases of volcanism spanning the Early Cretaceous to the Late Cretaceous. We believe the early lavas of the Hikurangi Plateau, in the form of laterally coherent dipping reflectors, are not overprinted by rifting and Late Cretaceous intraplate volcanism in the Pegasus Basin. These units may have been disrupted by Early Cretaceous rifting along the northern segment of the Hikurangi margin.
- (2) We imaged the pre-seamount basement interface, Horizon B, in several locations along the Hikurangi Trough. Based on its distribution, we interpret that a thick volcaniclastic Hikurangi Plateau unit exists along the central and northern Hikurangi Plateau, but it is substantially thinner or does not exist to the south in the Pegasus Basin. Much of the volcaniclastic sediments are associated with broad debris fans that emanate from large seamounts. This volcaniclastic cover is likely more fluid-rich than normal oceanic crust.
- (3) Large seamounts are observed along the Hikurangi Plateau outboard of the Hikurangi margin and east of the Hikurangi Trough, from the Rapuhia Scarp to the Chatham Rise. However, none are observed along the southern Hikurangi margin within the Pegasus Basin.
- (4) Small volcanic cones and sills surround and cap Māhia Seamount offshore Hawke Bay and the Māhia peninsula, and less so around Tūranganui Knoll. Dredged basanite lavas on Māhia Seamount date these neovolcanics as Pliocene. Due to the lack of a nearby hotspot, we suggest that these neovolcanics are petit-spot eruptions sourced from intraplate volcanism in response to the displacement and accumulation of hydrous melts derived from the mantle transition zone of the Pacific Plate.
- (5) Although small-throw normal faults are widespread in carbonate-rich sediments and the Hikurangi Plateau, we find limited evidence of contemporary outer-rise flexural normal faults outboard of the Hikurangi subduction zone. The only exception we observe is near Māhia Seamount, which could be linked to petit-spot volcanism. Thus, slab hydration from pervasive plate bending is not expected to be an important process before subduction, and any alteration of the Hikurangi Plateau may reflect ancient deformation and hydration events.
- (6) Because large seamounts and thick volcaniclastic deposits are not observed in the Pegasus Basin, we suggest that the effects of seamounts on slip processes in the Hikurangi margin are more dominant along the margin's

northern and central segments. These include influences of volcanic lithologies and topography on friction, roughness, and fluid delivery to the megathrust.

ACKNOWLEDGMENTS

We thank the officers, crew, and technical staff of the R/V Marcus G. Langseth for their efforts to collect the SHIRE multichannel seismic data. Maps were drafted with Generic Mapping Tools 6 (Wessel et al., 2019). Marine seismic data were processed with Paradigm software (https://www.pdgm.com). This research was supported by a National Science Foundation grant (NSF-EAR-1615815). Seismic basement horizon grids can be downloaded at https://zenodo.org/records/10779482. Marine multichannel seismic from the SHIRE project are available through the Marine Geoscience Data System (http://www.marine-geo.org/collections/). We are grateful to the reviewers and journal editors for providing constructive comments.

REFERENCES CITED

- Acquisto, T., Bécel, A., Singh, S.C., and Carton, H., 2022, Evidence of strong upper oceanic crustal hydration outboard the Alaskan and Sumatran subduction zones: Journal of Geophysical Research: Solid Earth, v. 127, https://doi.org/10.1029/2022JB024751.
- Allen, S.M., Marsaglia, K.M., Morgan, J., and Franco, A., 2022, Origin and diagenetic priming of a potential slow-slip trigger zone in volcanicilastic deposits flanking a seamount on the subducting plate, Hikurangi margin, New Zealand: New Zealand Journal of Geology and Geophysics, v. 65, p. 179–200, https://doi.org/10.1080/00288306.2021.1975776.
- Almeida, J., Riel, N., Rosas, F.M., Duarte, J.C., and Kaus, B., 2022, Self-replicating subduction zone initiation by polarity reversal: Communications Earth & Environment, v. 3, 55, https://doi.org/10.1038/s43247-022-00380-2.
- Anderson, D.L., 2005, Large igneous provinces, delamination, and fertile mantle: Elements, v. 1, p. 271–275, https://doi.org/10.2113/gselements.1.5.271.
- Andjić, G., Baumgartner, P.O., and Baumgartner-Mora, C., 2018, Rapid vertical motions and formation of volcanic arc gaps: Plateau collision recorded in the forearc geological evolution (Costa Rica margin): Basin Research, v. 30, p. 863–894, https://doi.org/10.1111/bre.12284.
- Arai, R., Kodaira, S., Yamada, T., Takahashi, T., Miura, S., Kaneda, Y., Nishizawa, A., and Oikawa, M., 2017, Subduction of thick oceanic plateau and high-angle normal-fault earthquakes intersecting the slab: Geophysical Research Letters, v. 44, p. 6109–6115, https://doi.org/10.1002/2017GL073789.
- Arai, R., et al., 2020, Three-dimensional P wave velocity structure of the northern Hikurangi margin from the NZ3D experiment: Evidence for fault-bound anisotropy: Journal of Geophysical Research: Solid Earth, v. 125, https://doi.org/10.1029/2020JB020433.
- Arnulf, A.F., Biemiller, J., Lavier, L., Wallace, L.M., Bassett, D., Henrys, S., Pecher, I., Crutchley, G., and Plaza Faverola, A., 2021, Physical conditions and frictional properties in the source region of a slow-slip event: Nature Geoscience, v. 14, p. 334–340, https://doi.org/10.1038/s41561-021-00741-0.
- Bangs, N.L., et al., 2023, Slow slip along the Hikurangi margin linked to fluid-rich sediments trailing subducting seamounts: Nature Geoscience, v. 16, p. 505–512, https://doi.org/10.1038/s41561-023-01186-3.
- Bangs, N.L.B., Gulick, S.P.S., and Shipley, T.H., 2006, Seamount subduction erosion in the Nankai Trough and its potential impact on the seismogenic zone: Geology, v. 34, p. 701–704, https://doi.org/10.1130/G22451.1.
- Bangs, N.L.B., McIntosh, K.D., Silver, E.A., Kluesner, J.W., and Ranero, C.R., 2015, Fluid accumulation along the Costa Rica subduction thrust and development of the seismogenic zone: Journal of Geophysical Research: Solid Earth, v. 120, p. 67–86, https://doi.org/10.1002/2014JB011265.
- Barker, D.H.N., Sutherland, R., Henrys, S., and Bannister, S., 2009, Geometry of the Hikurangi subduction thrust and upper plate, North Island, New Zealand: Geochemistry, Geophysics, Geosystems, v. 10, https://doi.org/10.1029/2008GC002153.
- Barker, D.H.N., Henrys, S., Caratori Tontini, F., Barnes, P.M., Bassett, D., Todd, E., and Wallace, L., 2018, Geophysical constraints on the relationship between seamount subduction, slow slip, and tremor at the north Hikurangi subduction zone, New Zealand: Geophysical Research Letters, v. 45, p. 12,804–12,813, https://doi.org/10.1029/2018GL080259.

- Barnes, P.M., Lamarche, G., Bialas, J., Henrys, S., Pecher, I., Netzeband, G.L., Greinert, J., Mountjoy, J.J., Pedley, K., and Crutchley, G., 2010, Tectonic and geological framework for gas hydrates and cold seeps on the Hikurangi subduction margin, New Zealand: Marine Geology, v. 272, p. 26–48, https://doi.org/10.1016/j.margeo.2009.03.012.
- Barnes, P.M., Ghisetti, F.C., Ellis, S., and Morgan, J.K., 2018, The role of protothrusts in frontal accretion and accommodation of plate convergence, Hikurangi subduction margin, New Zealand: Geosphere, v. 14, p. 440–468, https://doi.org/10.1130/GES01552.1.
- Barnes, P.M., et al., 2019, Site U1520, in Hikurangi Subduction Margin Coring, Logging, and Observatories: Proceedings of the International Ocean Discovery Program, v. 372B, no. 375, https://doi.org/10.14379/iodp.proc.372B375.105.2019.
- Barnes, P.M., et al., 2020, Slow slip source characterized by lithological and geometric heterogeneity: Science Advances, v. 6, https://doi.org/10.1126/sciadv.aay3314.
- Bassett, D., and Watts, A.B., 2015, Gravity anomalies, crustal structure, and seismicity at subduction zones: 1. Seafloor roughness and subducting relief: Geochemistry, Geophysics, Geosystems, v. 16. p. 1508–1540. https://doi.org/10.1002/2014GC005684.
- Bassett, D., Sutherland, R., Henrys, S., Stern, T., Scherwath, M., Benson, A., Toulmin, S., and Henderson, M., 2010, Three-dimensional velocity structure of the northern Hikurangi margin, Raukumara, New Zealand: Implications for the growth of continental crust by subduction erosion and tectonic underplating: Geochemistry, Geophysics, Geosystems, v. 11, https://doi .org/10.1029/2010GC003137.
- Bassett, D., Sutherland, R., and Henrys, S., 2014, Slow wave speeds and fluid overpressure in a region of shallow geodetic locking and slow slip, Hikurangi subduction margin, New Zealand: Earth and Planetary Science Letters, v. 389, p. 1–13, https://doi.org/10.1016/j.epsl.2013.12.021.
- Bassett, D., et al., 2022, Crustal structure of the Hikurangi margin from SHIRE seismic data and the relationship between forearc structure and shallow megathrust slip behavior: Geophysical Research Letters, v. 49, p. 1–11, https://doi.org/10.1029/2021GL096960.
- Bassett, D., et al., 2023, Heterogeneous crustal structure of the Hikurangi Plateau revealed by SHIRE seismic data: Origin and implications for plate boundary tectonics: Geophysical Research Letters, v. 50, https://doi.org/10.1029/2023GL105674.
- Bayona, G., Cardona, A., Jaramillo, C., Mora, A., Montes, C., Valencia, V., Ayala, C., Montenegro, O., and Ibañez-Mejia, M., 2012, Early Paleogene magmatism in the northern Andes: Insights on the effects of Oceanic Plateau-continent convergence: Earth and Planetary Science Letters, v. 331–332, p. 97–111, https://doi.org/10.1016/j.epsl.2012.03.015.
- Bell, R., Sutherland, R., Barker, D.H.N., Henrys, S., Bannister, S., Wallace, L., and Beavan, J., 2010, Seismic reflection character of the Hikurangi subduction interface, New Zealand, in the region of repeated Gisborne slow slip events: Geophysical Journal International, v. 180, p. 34–48, https://doi.org/10.1111/j.1365-246X.2009.04401.x.
- Bell, R., Holden, C., Power, W., Wang, X., and Downes, G., 2014, Hikurangi margin tsunami earth-quake generated by slow seismic rupture over a subducted seamount: Earth and Planetary Science Letters, v. 397, p. 1–9, https://doi.org/10.1016/j.epsl.2014.04.005.
- Billen, M.I., and Stock, J., 2000, Morphology and origin of the Osbourn Trough: Journal of Geophysical Research: Solid Earth, v. 105, p. 13,481–13,489, https://doi.org/10.1029/2000JB900035.
- Bland, K.J., Uruski, C.I., and Isaac, M.J., 2015, Pegasus Basin, eastern New Zealand: A stratigraphic record of subsidence and subduction, ancient and modern: New Zealand Journal of Geology and Geophysics, v. 58, p. 319–343, https://doi.org/10.1080/00288306.2015.1076862.
- Bonnet, G., Agard, P., Angiboust, S., Fournier, M., and Omrani, J., 2019, No large earthquakes in fully exposed subducted seamount: Geology, v. 47, p. 407–410, https://doi.org/10.1130 /G45564.1.
- Bonnet, G., Agard, P., Angiboust, S., Monié, P., Fournier, M., Caron, B., and Omrani, J., 2020, Structure and metamorphism of a subducted seamount (Zagros suture, Southern Iran): Geosphere, v. 16, p. 62–81, https://doi.org/10.1130/GES02134.1.
- Boulton, C., Niemeijer, A.R., Hollis, C.J., Townend, J., Raven, M.D., Kulhanek, D.K., and Shepherd, C.L., 2019, Temperature-dependent frictional properties of heterogeneous Hikurangi subduction zone input sediments, ODP Site 1124: Tectonophysics, v. 757, p. 123–139, https://doi.org/10.1016/j.tecto.2019.02.006.
- Buchs, D.M., Baumgartner, P.O., Baumgartner-Mora, C., Bandini, A.N., Jackett, S.-J., Diserens, M.-O., and Stucki, J., 2009, Late Cretaceous to Miocene seamount accretion and mélange formation in the Osa and Burica Peninsulas (Southern Costa Rica): Episodic growth of a convergent margin, in James, K.H., Lorente, M.A., and Pindell, J.L., eds., The Origin and Evolution of the Caribbean Plate: Geological Society, London, Special Publication 328, p. 411–456, https://doi.org/10.1144/SP328.17.

- Buchs, D.M., Arculus, R.J., Baumgartner, P.O., and Ulianov, A., 2011, Oceanic intraplate volcanoes exposed: Example from seamounts accreted in Panama: Geology, v. 39, p. 335–338, https:// doi.org/10.1130/G31703.1.
- Buchs, D.M., Pilet, S., Cosca, M., Flores, K.E., Bandini, A.N., and Baumgartner, P.O., 2013, Low-volume intraplate volcanism in the Early/Middle Jurassic Pacific basin documented by accreted sequences in Costa Rica: Geochemistry, Geophysics, Geosystems, v. 14, p. 1552–1568, https://doi.org/10.1002/ggge.20084.
- Carr, M.J., Feigenson, M.D., Patino, L.C., and Walker, J.A., 2003, Volcanism and geochemistry in Central America: Progress and problems, in Eiler, J., ed., Inside the Subduction Factory: American Geophysical Union, Geophysical Monograph Series, v. 138, p. 153–174, https://doi.org/10.1029/138GM09.
- Chandler, M.T., Wessel, P., Taylor, B., Seton, M., Kim, S.-S., and Hyeong, K., 2012, Reconstructing Ontong Java Nui: Implications for Pacific absolute plate motion, hotspot drift and true polar wander: Earth and Planetary Science Letters, v. 331–332, p. 140–151, https://doi.org/10.1016/j.epsl.2012.03.017.
- Chen, Y.J., 1992, Oceanic crustal thickness versus spreading rate: Geophysical Research Letters, v. 19, p. 753–756, https://doi.org/10.1029/92GL00161.
- Chesley, C., Naif, S., Key, K., and Bassett, D., 2021, Fluid-rich subducting topography generates anomalous forearc porosity: Nature, v. 595, p. 255–260, https://doi.org/10.1038/s41586-021-03619-8.
- Chlieh, M., Perfettini, H., Tavera, H., Avouac, J.-P., Remy, D., Nocquet, J.-M., Rolandone, F., Bondoux, F., Gabalda, G., and Bonvalot, S., 2011, Interseismic coupling and seismic potential along the Central Andes subduction zone: Journal of Geophysical Research: Solid Earth, v. 116, https://doi.org/10.1029/2010JB008166.
- Chlieh, M., et al., 2014, Distribution of discrete seismic asperities and aseismic slip along the Ecuadorian megathrust: Earth and Planetary Science Letters, v. 400, p. 292–301, https://doi.org/10.1016/j.epsl.2014.05.027.
- Chow, B., Kaneko, Y., and Townend, J., 2022, Evidence for deeply subducted lower-plate seamounts at the Hikurangi subduction margin: Implications for seismic and aseismic behavior: Journal of Geophysical Research: Solid Earth, v. 127, p. 1–21, https://doi.org/10.1029/2021JB022866.
- Christeson, G.L., Goff, J.A., and Reece, R.S., 2019, Synthesis of oceanic crustal structure from two-dimensional seismic profiles: Reviews of Geophysics, v. 57, p. 504–529, https://doi.org /10.1029/2019RG000641.
- Clarke, A.P., Vannucchi, P., and Morgan, J., 2018, Seamount chain-subduction zone interactions: Implications for accretionary and erosive subduction zone behavior: Geology, v. 46, p. 367–370, https://doi.org/10.1130/G40063.1.
- Cloos, M., 1992, Thrust-type subduction-zone earthquakes and seamount asperities: A physical model for seismic rupture: Geology, v. 20, p. 601–604, https://doi.org/10.1130/0091-7613 (1992)020<0601:TTSZEA>2.3.CO:2.
- Cloos, M., 1993, Lithospheric buoyancy and collisional orogenesis: Subduction of oceanic plateaus, continental margins, island arcs, spreading ridges, and seamounts: Geological Society of America Bulletin, v. 105, p. 715–737, https://doi.org/10.1130/0016-7606(1993)105<0715:LBA COS>2.3.CO;2.
- Coffin, M.F., and Eldholm, O., 1994, Large igneous provinces: Crustal structure, dimensions, and external consequences: Reviews of Geophysics, v. 32, p. 1–36, https://doi.org/10.1029/93RG02508.
- Collot, J., and Davy, B., 1998, Forearc structures and tectonic regimes at the oblique subduction zone between the Hikurangi Plateau and the southern Kermadec margin: Journal of Geophysical Research: Solid Earth, v. 103, p. 623–650, https://doi.org/10.1029/97JB02474.
- Collot, J.-Y., Lewis, K., Lamarche, G., and Lallemand, S., 2001, The giant Ruatoria debris avalanche on the northern Hikurangi margin, New Zealand: Result of oblique seamount subduction: Journal of Geophysical Research: Solid Earth, v. 106, p. 19,271–19,297, https://doi.org/10.1029/2001JB900004.
- Collot, J.-Y., Sanclemente, E., Nocquet, J.-M., Leprêtre, A., Ribodetti, A., Jarrin, P., Chlieh, M., Graindorge, D., and Charvis, P., 2017, Subducted oceanic relief locks the shallow megathrust in central Ecuador: Journal of Geophysical Research: Solid Earth, v. 122, p. 3286–3305, https:// doi.org/10.1002/2016JB013849.
- Contreras-Reyes, E., and Carrizo, D., 2011, Control of high oceanic features and subduction channel on earthquake ruptures along the Chile–Peru subduction zone: Physics of the Earth and Planetary Interiors, v. 186, p. 49–58, https://doi.org/10.1016/j.pepi.2011.03.002.
- Contreras-Reyes, E., Cortés-Rivas, V., Manríquez, P., and Maksymowicz, A., 2021, The silent bending of the oceanic Nazca Plate at the Peruvian Trench: Tectonophysics, v. 807, https://doi.org/10.1016/j.tecto.2021.228810.

- Crampton, J.S., Mortimer, N., Bland, K.J., Strogen, D.P., Sagar, M., Hines, B.R., King, P.R., and Seebeck, H., 2019, Cretaceous termination of subduction at the Zealandia margin of Gondwana: The view from the paleo-trench: Gondwana Research, v. 70, p. 222–242, https://doi.org/10.1016/j.gr.2019.01.010.
- Crutchley, G.J., Klaeschen, D., Henrys, S.A., Pecher, I.A., Mountjoy, J.J., and Woelz, S., 2020, Subducted sediments, upper-plate deformation and dewatering at New Zealand's southern Hikurangi subduction margin: Earth and Planetary Science Letters, v. 530, https://doi .org/10.1016/j.epsl.2019.115945.
- Davidson, S.R., Barnes, P.M., Pettinga, J.R., Nicol, A., Mountjoy, J.J., and Henrys, S.A., 2020, Conjugate strike-slip faulting across a subduction front driven by incipient seamount subduction: Geology, v. 48, p. 493–498, https://doi.org/10.1130/G47154.1.
- Davy, B., 2014, Rotation and offset of the Gondwana convergent margin in the New Zealand region following Cretaceous jamming of Hikurangi Plateau large igneous province subduction: Tectonics, v. 33, p. 1577–1595, https://doi.org/10.1002/2014TC003629.
- Davy, B., and Collot, J.-Y., 2000, The Rapuhia Scarp (northern Hikurangi Plateau) Its nature and subduction effects on the Kermadec Trench: Tectonophysics, v. 328, p. 269–295, https://doi. org/10.1016/S0040-1951(00)00211-0.
- Davy, B., and Wood, R., 1994, Gravity and magnetic modelling of the Hikurangi Plateau: Marine Geology, v. 118, p. 139–151, https://doi.org/10.1016/0025-3227(94)90117-1.
- Davy, B., Hoernle, K., and Werner, R., 2008, Hikurangi Plateau: Crustal structure, rifted formation, and Gondwana subduction history: Geochemistry, Geophysics, Geosystems, v. 9, https://doi.org/10.1029/2007GC001855.
- DeMets, C., Gordon, R.G., and Argus, D.F., 2010, Geologically current plate motions: Geophysical Journal International, v. 181, p. 1–80, https://doi.org/10.1111/j.1365-246X.2009.04491.x.
- Dominguez, S., Malavieille, J., and Lallemand, S.E., 2000, Deformation of accretionary wedges in response to seamount subduction: Insights from sandbox experiments: Tectonics, v. 19, p. 182–196, https://doi.org/10.1029/1999TC900055.
- Ellis, S., Beaumont, C., and Pfiffner, O.A., 1999, Geodynamic models of crustal-scale episodic tectonic accretion and underplating in subduction zones: Journal of Geophysical Research: Solid Earth, v. 104, p. 15,169–15,190, https://doi.org/10.1029/1999JB900071.
- Ellis, S., Fagereng, Å., Barker, D., Henrys, S., Saffer, D., Wallace, L., Williams, C., and Harris, R., 2015, Fluid budgets along the northern Hikurangi subduction margin, New Zealand: The effect of a subducting seamount on fluid pressure: Geophysical Journal International, v. 202, p. 277–297, https://doi.org/10.1093/gji/ggv127.
- Fagereng, Å., 2011, Wedge geometry, mechanical strength, and interseismic coupling of the Hikurangi subduction thrust, New Zealand: Tectonophysics, v. 507, p. 26–30, https://doi.org/10.1016/j.tecto.2011.05.004.
- Fagereng, Å., and Beall, A., 2021, Is complex fault zone behaviour a reflection of rheological heterogeneity?: Philosophical Transactions of the Royal Society A: Mathematical, Physical and Engineering Sciences, v. 379, https://doi.org/10.1098/rsta.2019.0421.
- Fagereng, Å., and Sibson, R.H., 2010, Mélange rheology and seismic style: Geology, v. 38, p. 751–754, https://doi.org/10.1130/G30868.1.
- Frederik, M.C.G., Gulick, S.P.S., and Miller, J.J., 2020, Effect on subduction of deeply buried seamounts offshore of Kodiak Island: Tectonics, v. 39, p. 1–14, https://doi.org/10.1029/2019TC005710.
- Fujie, G., Kodaira, S., Nakamura, Y., Morgan, J.P., Dannowski, A., Thorwart, M., Grevemeyer, I., and Miura, S., 2020, Spatial variations of incoming sediments at the northeastern Japan arc and their implications for megathrust earthquakes: Geology, v. 48, p. 614–619, https://doi. org/10.1130/G46757.1.
- Gase, A.C., et al., 2021, Crustal structure of the Northern Hikurangi margin, New Zealand: Variable accretion and overthrusting plate strength influenced by rough subduction: Journal of Geophysical Research: Solid Earth, v. 126, p. 1–26, https://doi.org/10.1029/2020JB021176.
- Gase, A.C., Bangs, N.L., Van Avendonk, H.J.A., Bassett, D., and Henrys, S.A., 2022, Hikurangi megathrust slip behavior influenced by lateral variability in sediment subduction: Geology, v. 50, p. 1145–1149, https://doi.org/10.1130/G50261.1.
- Gase, A.C., et al., 2023, Subducting volcaniclastic-rich upper crust supplies fluids for shallow megathrust and slow slip: Science Advances, v. 9, https://doi.org/10.1126/sciadv.adh0150.
- Geersen, J., Ranero, C.R., Barckhausen, U., and Reichert, C., 2015, Subducting seamounts control interplate coupling and seismic rupture in the 2014 Iquique earthquake area: Nature Communications, v. 6, 8267, https://doi.org/10.1038/ncomms9267.
- Ghisetti, F.C., Barnes, P.M., Ellis, S., Plaza-Faverola, A.A., and Barker, D.H.N., 2016, The last 2 Myr of accretionary wedge construction in the central Hikurangi margin (North Island, New

- Zealand): Insights from structural modeling: Geochemistry, Geophysics, Geosystems, v. 17, p. 2661–2686, https://doi.org/10.1002/2016GC006341.
- Gray, M., Bell, R.E., Morgan, J.V., Henrys, S., and Barker, D.H.N., 2019, Imaging the shallow subsurface structure of the North Hikurangi subduction zone, New Zealand, using 2-D full-waveform inversion: Journal of Geophysical Research: Solid Earth, v. 124, p. 9049–9074, https://doi.org/10.1029/2019.JB017793.
- Grevemeyer, I., Ranero, C.R., and Ivandic, M., 2018, Structure of oceanic crust and serpentinization at subduction trenches: Geosphere, v. 14, p. 395–418, https://doi.org/10.1130/GES01537.1.
- Gulick, S.P.S., Lowe, L.A., Pavlis, T.L., Gardner, J.V., and Mayer, L.A., 2007, Geophysical insights into the Transition fault debate: Propagating strike slip in response to stalling Yakutat block subduction in the Gulf of Alaska: Geology, v. 35, p. 763–766, https://doi.org/10.1130/G23585A.1.
- Gün, E., Pysklywec, R.N., Topuz, G., Oğuz, H.G., and Heron, P.J., 2024, Syn-drift plate tectonics: Geophysical Research Letters, v. 51, p. 1–9, https://doi.org/10.1029/2023GL105452.
- Han, S., Carbotte, S.M., Canales, J.P., Nedimović, M.R., and Carton, H., 2018, Along-trench structural variations of the subducting Juan de Fuca Plate from multichannel seismic reflection imaging: Journal of Geophysical Research: Solid Earth, v. 123, p. 3122–3146, https://doi.org/10.1002/2017.JB015059.
- Henrys, S., Reyners, M., Pecher, I., Bannister, S., Nishimura, Y., and Maslen, G., 2006, Kinking of the subducting slab by escalator normal faulting beneath the North Island of New Zealand: Geology, v. 34, p. 777–780, https://doi.org/10.1130/G22594.1.
- Henrys, S., et al., 2013, SAHKE geophysical transect reveals crustal and subduction zone structure at the southern Hikurangi margin, New Zealand: Geochemistry, Geophysics, Geosystems, v. 14, p. 2063–2083, https://doi.org/10.1002/ggge.20136.
- Herath, P., Stern, T.A., Savage, M.K., Bassett, D., Henrys, S., and Boulton, C., 2020, Hydration of the crust and upper mantle of the Hikurangi Plateau as it subducts at the southern Hikurangi margin: Earth and Planetary Science Letters, v. 541, https://doi.org/10.1016/j.epsl.2020.116271.
- Herath, P., Stern, T.A., Savage, M.K., Bassett, D., and Henrys, S., 2022, Wide-angle seismic reflections reveal a lithosphere-asthenosphere boundary zone in the subducting Pacific Plate, New Zealand: Science Advances, v. 8, p. 1–10, https://doi.org/10.1126/sciadv.abn5697.
- Hirano, N., and Machida, S., 2022, The mantle structure below petit-spot volcanoes: Communications Earth & Environment, v. 3, 110, https://doi.org/10.1038/s43247-022-00438-1.
- Hirano, N., Kawamura, K., Hattori, M., Saito, K., and Ogawa, Y., 2001, A new type of intra-plate volcanism; young alkali-basalts discovered from the subducting Pacific Plate, Northern Japan Trench: Geophysical Research Letters, v. 28, p. 2719–2722, https://doi.org/10.1029/2000GL012426.
- Hirano, N., et al., 2006, Volcanism in response to plate flexure: Science, v. 313, p. 1426–1428, https://doi.org/10.1126/science.1128235.
- Hirano, N., Koppers, A.A.P., Takahashi, A., Fujiwara, T., and Nakanishi, M., 2008, Seamounts, knolls and petit-spot monogenetic volcanoes on the subducting Pacific Plate: Basin Research, v. 20, p. 543–553, https://doi.org/10.1111/j.1365-2117.2008.00363.x.
- Hochmuth, K., Gohl, K., Uenzelmann-Neben, G., and Werner, R., 2019, Multiphase magmatic and tectonic evolution of a large igneous province—Evidence from the crustal structure of the Manihiki Plateau, western Pacific: Tectonophysics, v. 750, p. 434–457, https://doi.org/10.1016/j tecto. 2018 11.014
- Hoernle, K., Hauff, F., Werner, R., and Mortimer, N., 2004, New insights into the origin and evolution of the Hikurangi oceanic plateau: Eos (Transactions, American Geophysical Union), v. 85, p. 401–408. https://doi.org/10.1029/2004EO410001.
- Hoernle, K., Hauff, F., van den Bogaard, P., Werner, R., Mortimer, N., Geldmacher, J., Garbe-Schönberg, D., and Davy, B., 2010, Age and geochemistry of volcanic rocks from the Hikurangi and Manihiki oceanic plateaus: Geochimica et Cosmochimica Acta, v. 74, p. 7196–7219, https://doi.org/10.1016/j.gca.2010.09.030.
- Hoernle, K., Hauff, F., Werner, R., van den Bogaard, P., Gibbons, A.D., Conrad, S., and Müller, R.D., 2011, Origin of Indian Ocean Seamount Province by shallow recycling of continental lithosphere: Nature Geoscience, v. 4, p. 883–887, https://doi.org/10.1038/ngeo1331.
- Hoernle, K., Timm, C., Hauff, F., Tappenden, V., Werner, R., Jolis, E.M., Mortimer, N., Weaver, S., Riefstahl, F., and Gohl, K., 2020, Late Cretaceous (99–69 Ma) basaltic intraplate volcanism on and around Zealandia: Tracing upper mantle geodynamics from Hikurangi Plateau collision to Gondwana breakup and beyond: Earth and Planetary Science Letters, v. 529, https://doi .org/10.1016/j.epsl.2019.115864.
- Homrighausen, S., Hoernle, K., Geldmacher, J., Wartho, J.-A., Hauff, F., Portnyagin, M., Werner, R., van den Bogaard, P., and Garbe-Schönberg, D., 2018, Unexpected HIMU-type late-stage volcanism on the Walvis Ridge: Earth and Planetary Science Letters, v. 492, p. 251–263, https://doi.org/10.1016/j.epsl.2018.03.049.

- Horton, B.K., Capaldi, T.N., and Perez, N.D., 2022, The role of flat slab subduction, ridge subduction, and tectonic inheritance in Andean deformation: Geology, v. 50, p. 1007–1012, https://doi.org/10.1130/G50094.1.
- Humphreys, E., 2009, Relation of flat subduction to magmatism and deformation in the western United States, in Mahlburg Kay, S., Ramos, V.A., and Dickinson, W.R., Backbone of the Americas: Shallow Subduction, Plateau Uplift, and Ridge and Terrane Collision: Geological Society of America Memoir 204, p. 85–98, https://doi.org/10.1130/2009.1204(04).
- lkari, M.J., Marone, C., and Saffer, D.M., 2011, On the relation between fault strength and frictional stability: Geology, v. 39, p. 83–86, https://doi.org/10.1130/G31416.1.
- Ikari, M.J., Marone, C., Saffer, D.M., and Kopf, A.J., 2013, Slip weakening as a mechanism for slow earthquakes: Nature Geoscience, v. 6, p. 468–472, https://doi.org/10.1038/ngeo1818.
- Im, K., Saffer, D., Marone, C., and Avouac, J.-P., 2020, Slip-rate-dependent friction as a universal mechanism for slow slip events: Nature Geoscience, v. 13, p. 705–710, https://doi.org/10.1038 /s41561-020-0627-9.
- Ingle, S., and Coffin, M.F., 2004, Impact origin for the greater Ontong Java Plateau?: Earth and Planetary Science Letters, v. 218, p. 123–134, https://doi.org/10.1016/S0012-821X(03)00629-0.
- Inoue, H., Coffin, M.F., Nakamura, Y., Mochizuki, K., and Kroenke, L.W., 2008, Intrabasement reflections of the Ontong Java Plateau: Implications for plateau construction: Geochemistry, Geophysics, Geosystems, v. 9, p. 1–19, https://doi.org/10.1029/2007GC001780.
- Jackson, E.D., Bargar, K.E., Fabbi, B.P., and Heropoulos, C., 1976, Petrology of the basaltic rocks drilled on Leg 33 of the Deep Sea Drilling Project: Deep Sea Drilling Project Initial Reports Volume 33, p. 571–630, https://doi.org/10.2973/dsdp.proc.33.120.1976.
- Jenkyns, H.C., 1976, Sediments and sedimentary history, Manihiki Plateau, South Pacific Ocean: Deep Sea Drilling Project Initial Reports Volume 33, p. 873–890, https://doi.org/10.2973/dsdp.proc.33.134.1976.
- Kelleher, J., and McCann, W., 1976, Buoyant zones, great earthquakes, and unstable boundaries of subduction: Journal of Geophysical Research: Solid Earth and Planets, v. 81, p. 4885–4896, https://doi.org/10.1029/JB081i026p04885.
- Kim, S.-S., and Wessel, P., 2011, New global seamount census from altimetry-derived gravity data: Geophysical Journal International, v. 186, p. 615–631, https://doi.org/10.1111/j.1365 -246X.2011.05076.x.
- Kodaira, S., Takahashi, N., Nakanishi, A., Miura, S., and Kaneda, Y., 2000, Subducted seamount imaged in the rupture zone of the 1946 Nankaido earthquake: Science, v. 289, p. 104–106, https://doi.org/10.1126/science.289.5476.104.
- Koppers, A.A.P., et al., 2010, Massive basalt flows on the southern flank of Tamu Massif, Shatsky Rise: A reappraisal of ODP Site 1213 basement units, in Sager, W.W., Sano, T., Geldmacher, J., and the Expedition 324 Scientists, Proceedings of the Integrated Ocean Drilling Program, Volume 324: Tokyo, Integrated Ocean Drilling Program Management International, Inc., 20 p., https://doi.org/10.2204/jodp.proc.324.109.2010.
- Koppers, A.A.P., Gowen, M.D., Colwell, L.E., Gee, J.S., Lonsdale, P.F., Mahoney, J.J., and Duncan, R.A., 2011, New ⁶⁰Ar/⁶⁹Ar age progression for the Louisville hot spot trail and implications for inter-hot spot motion: Geochemistry, Geophysics, Geosystems, v. 12, https://doi.org/10.1029/2011GC003804.
- Korenaga, J., 2005, Why did not the Ontong Java Plateau form subaerially?: Earth and Planetary Science Letters, v. 234, p. 385–399, https://doi.org/10.1016/j.epsl.2005.03.011.
- Kurzawski, R.M., Stipp, M., Niemeijer, A.R., Spiers, C.J., and Behrmann, J.H., 2016, Earthquake nucleation in weak subducted carbonates: Nature Geoscience, v. 9, p. 717–722, https://doi .org/10.1038/ngeo2774.
- Lallemand, S., and Le Pichon, X., 1987, Coulomb wedge model applied to the subduction of seamounts in the Japan Trench: Geology, v. 15, p. 1065–1069, https://doi.org/10.1130/0091-7613 (1987)15
- Lallemand, S., Peyret, M., van Rijsingen, E., Arcay, D., and Heuret, A., 2018, Roughness characteristics of oceanic seafloor prior to subduction in relation to the seismogenic potential of subduction zones: Geochemistry, Geophysics, Geosystems, v. 19, p. 2121–2146, https://doi.org/10.1029/2018GC007434.
- Larson, R.L., 1991, Latest pulse of Earth: Evidence for a mid-Cretaceous superplume: Geology, v. 19, p. 547–550, https://doi.org/10.1130/0091-7613(1991)019<0547:LPOEEF>2.3.CO;2.
- Larson, R.L., 1997, Superplumes and ridge interactions between Ontong Java and Manihiki Plateaus and the Nova-Canton Trough: Geology, v. 25, p. 779–782, https://doi.org/10.1130/0091-7613(1997)025<0779:SARIBO>2.3.CO;2.
- Leah, H., Fagereng, Å., Bastow, I., Bell, R., Lane, V., Henrys, S., Jacobs, K., and Fry, B., 2022, The northern Hikurangi margin three-dimensional plate interface in New Zealand remains rough 100 km from the trench: Geology, v. 50, p. 1256–1260, https://doi.org/10.1130/G50272.1.

- Lee, S., Choi, E., and Scholz, C.H., 2023, Do subducted seamounts act as weak asperities?: Journal of Geophysical Research: Solid Earth, v. 128, p. 1–14, https://doi.org/10.1029/2023JB027551.
- Leeman, J.R., Saffer, D.M., Scuderi, M.M., and Marone, C., 2016, Laboratory observations of slow earthquakes and the spectrum of tectonic fault slip modes: Nature Communications, v. 7, https://doi.org/10.1038/ncomms11104.
- Leslie, S.C., Moore, G.F., Morgan, J.K., and Hills, D.J., 2002, Seismic stratigraphy of the Frontal Hawaiian Moat: Implications for sedimentary processes at the leading edge of an oceanic hotspot trace: Marine Geology, v. 184, p. 143–162, https://doi.org/10.1016/S0025-3227 (01)00284-5.
- Lewis, K.B., Collot, J., and Lallem, S.E., 1998, The dammed Hikurangi Trough: A channel-fed trench blocked by subducting seamounts and their wake avalanches (New Zealand–France GeodyNZ Project): Basin Research, v. 10, p. 441–468, https://doi.org/10.1046/j.1365-2117.1998.00080.x.
- Liu, L., Gurnis, M., Seton, M., Saleeby, J., Müller, R.D., and Jackson, J.M., 2010, The role of oceanic plateau subduction in the Laramide orogeny: Nature Geoscience, v. 3, p. 353–357, https://doi. org/10.1038/ngeo829.
- Liu, Y., and Rice, J.R., 2007, Spontaneous and triggered aseismic deformation transients in a subduction fault model: Journal of Geophysical Research: Solid Earth, v. 112, p. 1–23, https://doi.org/10.1029/2007JB004930.
- Machida, S., Hirano, N., Sumino, H., Hirata, T., Yoneda, S., and Kato, Y., 2015, Petit-spot geology reveals melts in upper-most asthenosphere dragged by lithosphere: Earth and Planetary Science Letters, v. 426, p. 267–279, https://doi.org/10.1016/j.epsl.2015.06.018.
- Mahoney, J.J., and Spencer, K.J., 1991, Isotopic evidence for the origin of the Manihiki and Ontong Java oceanic plateaus: Earth and Planetary Science Letters, v. 104, p. 196–210, https://doi.org/10.1016/0012-821X(91)90204-U.
- Mahoney, J.J., Storey, M., Duncan, R.A., Spencer, K.J., and Pringle, M., 1993, Geochemistry and geochronology of Leg 130 basement lavas: Nature and origin of the Ontong Java Plateau, in Berger, W.H., et al., 1993 Proceedings of the Ocean Drilling Program, Scientific Results, Volume 130: College Station, Texas, Ocean Drilling Program, p. 3–22, https://doi.org/10.2973 /odp.proc.sr.130.040.1993.
- Marcaillou, B., Collot, J.-Y., Ribodetti, A., D'Acremont, E., Mahamat, A.-A., and Alvarado, A., 2016, Seamount subduction at the North-Ecuadorian convergent margin: Effects on structures, inter-seismic coupling and seismogenesis: Earth and Planetary Science Letters, v. 433, p. 146– 158, https://doi.org/10.1016/j.epsl.2015.10.043.
- Martinez-Loriente, S., Sallarès, V.R., Ranero, C.B., Ruh, J., Barckhausen, U., Grevemeyer, I., and Bangs, N., 2019, Influence of incoming plate relief on overriding plate deformation and earthquake nucleation: Cocos Ridge subduction (Costa Rica): Tectonics, v. 38, p. 4360–4377, https:// doi.org/10.1029/2019TC005586.
- Mather, B.R., Müller, R.D., Seton, M., Ruttor, S., Nebel, O., and Mortimer, N., 2020, Intraplate volcanism triggered by bursts in slab flux: Science Advances, v. 6, p. 1–9, https://doi.org/10.1126/sciadv.abd0953.
- McArthur, A.D., and McCaffrey, W.D., 2019, Sedimentary architecture of detached deep-marine canyons: Examples from the East Coast Basin of New Zealand: Sedimentology, v. 66, p. 1067–1101, https://doi.org/10.1111/sed.12536.
- McArthur, A.D., Claussmann, B., Bailleul, J., Clare, A., and McCaffrey, W.D., 2020, Variation in syn-subduction sedimentation patterns from inner to outer portions of deep-water fold and thrust belts: Examples from the Hikurangi subduction margin of New Zealand, *in* Hammerstein, J.A., Di Cuia, R., Cottam, M.A., Zamora, G., and Butler, R.W.H., eds., Fold and Thrust Belts: Structural Style, Evolution and Exploration: Geological Society, London, Special Publication 490, p. 285–310, https://doi.org/10.1144/SP490-2018-95.
- Menant, A., Angiboust, S., Gerya, T., Lacassin, R., Simoes, M., and Grandin, R., 2020, Transient stripping of subducting slabs controls periodic forearc uplift: Nature Communications, v. 11, 1823, https://doi.org/10.1038/s41467-020-15580-7.
- Miller, N.C., Lizarralde, D., Collins, J.A., Holbrook, W.S., and Van Avendonk, H.J.A., 2021, Limited mantle hydration by bending faults at the Middle America Trench: Journal of Geophysical Research: Solid Earth, v. 126, https://doi.org/10.1029/2020JB020982.
- Miura, S., Suyehiro, K., Shinohara, M., Takahashi, N., Araki, E., and Taira, A., 2004, Seismological structure and implications of collision between the Ontong Java Plateau and Solomon Island Arc from ocean bottom seismometer-airgun data: Tectonophysics, v. 389, p. 191–220, https:// doi.org/10.1016/j.tecto.2003.09.029.
- Mochizuki, K., Yamada, T., Shinohara, M., Yamanaka, Y., and Kanazawa, T., 2008, Weak interplate coupling by seamounts and repeating M 7 earthquakes: Science, v. 321, p. 1194–1197, https://doi.org/10.1126/science.1160250.

- Mochizuki, K., et al., 2019, Recycling of depleted continental mantle by subduction and plumes at the Hikurangi Plateau large igneous province, southwestern Pacific Ocean: Geology, v. 47, p. 795–798, https://doi.org/10.1130/G46250.1.
- Mochizuki, K., Henrys, S., Haijima, D., Warren-Smith, E., and Fry, B., 2021, Seismicity and velocity structure in the vicinity of repeating slow slip earthquakes, northern Hikurangi subduction zone, New Zealand: Earth and Planetary Science Letters, v. 563, https://doi.org/10.1016/j.epsl.2021.116887.
- Morgan, J.K., and Bangs, N.L., 2017, Recognizing seamount-forearc collisions at accretionary margins: Insights from discrete numerical simulations: Geology, v. 45, p. 635–638, https://doi.org/10.1130/G38923.1.
- Morgan, J.K., et al., 2022, Seafloor overthrusting causes ductile fault deformation and fault sealing along the northern Hikurangi margin: Earth and Planetary Science Letters, v. 593, https://doi.org/10.1016/j.epsl.2022.117651.
- Mortimer, N., Hoernle, K., Hauff, F., Palin, J.M., Dunlap, W.J., Werner, R., and Faure, K., 2006, New constraints on the age and evolution of the Wishbone Ridge, southwest Pacific Cretaceous microplates, and Zealandia–West Antarctica breakup: Geology, v. 34, p. 185–188, https://doi. org/10.1130/G22168.1.
- Mortimer, N., et al., 2018, Regional volcanism of northern Zealandia: Post-Gondwana break-up magmatism on an extended, submerged continent: Geological Society, London, Special Publication 463. p. 199–226. https://doi.org/10.1144/SP463.9.
- Mortimer, N., van den Bogaard, P., Hoernle, K., Timm, C., Gans, P.B., Werner, R., and Riefstahl, F., 2019, Late Cretaceous oceanic plate reorganization and the breakup of Zealandia and Gondwana: Gondwana Research, v. 65, p. 31–42, https://doi.org/10.1016/j.gr.2018.07.010.
- Mortimer, N., Campbell, H.J., and Moerhuis, N., 2020, Chatham Schist: New Zealand Journal of Geology and Geophysics, v. 63, p. 237–249, https://doi.org/10.1080/00288306
- Myers, E.K., Roland, E.C., Tréhu, A.M., and Davenport, K., 2022, Crustal structure of the incoming lquique Ridge offshore Northern Chile: Journal of Geophysical Research: Solid Earth, v. 127, p. 1–20, https://doi.org/10.1029/2021JB023169.
- Naif, S., Key, K., Constable, S., and Evans, R.L., 2015, Water-rich bending faults at the Middle America Trench: Geochemistry, Geophysics, Geosystems, v. 16, p. 2582–2597, https://doi.org/10.1002/2015GC005927.
- Naif, S., Miller, N.C., Shillington, D.J., Bécel, A., Lizarralde, D., Bassett, D., and Hemming, S.R., 2023, Episodic intraplate magmatism fed by a long-lived melt channel of distal plume origin: Science Advances, v. 9, https://doi.org/10.1126/sciadv.add3761.
- Nicol, A., Mazengarb, C., Chanier, F., Rait, G., Uruski, C., and Wallace, L., 2007, Tectonic evolution of the active Hikurangi subduction margin, New Zealand, since the Oligocene: Tectonics, v. 26, p. 1–24, https://doi.org/10.1029/2006TC002090.
- Nishimura, T., 2014, Short-term slow slip events along the Ryukyu Trench, southwestern Japan, observed by continuous GNSS: Progress in Earth and Planetary Science, v. 1, 22, https://doi.org/10.1186/s40645-014-0022-5.
- Ohira, A., Kodaira, S., Fujie, G., No, T., Nakamura, Y., Kaiho, Y., and Miura, S., 2018, Seismic structure of the oceanic crust around petit-spot volcanoes in the outer-rise region of the Japan Trench: Geophysical Research Letters, v. 45, p. 11,123–11,129, https://doi.org/10.1029/2018GL080305.
- Park, J.-O., Tsuru, T., Kaneda, Y., Kono, Y., Kodaira, S., Takahashi, N., and Kinoshita, H., 1999, A subducting seamount beneath the Nankai Accretionary Prism off Shikoku, southwestern Japan: Geophysical Research Letters, v. 26, p. 931–934, https://doi.org/10.1029 /1999GL900134.
- Park, J.-O., Moore, G.F., Tsuru, T., Kodaira, S., and Kaneda, Y., 2004, A subducted oceanic ridge influencing the Nankai megathrust earthquake rupture: Earth and Planetary Science Letters, v. 217, p. 77–84, https://doi.org/10.1016/S0012-821X(03)00553-3.
- Parsiegla, N., Gohl, K., and Uenzelmann-Neben, G., 2008, The Agulhas Plateau: Structure and evolution of a large igneous province: Geophysical Journal International, v. 174, p. 336–350, https://doi.org/10.1111/j.1365-246X.2008.03808.x.
- Pedley, K.L., Barnes, P.M., Pettinga, J.R., and Lewis, K.B., 2010, Seafloor structural geomorphic evolution of the accretionary frontal wedge in response to seamount subduction, Poverty Indentation, New Zealand: Marine Geology, v. 270, p. 119–138, https://doi.org/10.1016/j .margeo.2009.11.006.
- Pietsch, R., and Uenzelmann-Neben, G., 2015, The Manihiki Plateau—A multistage volcanic emplacement history: Geochemistry, Geophysics, Geosystems, v. 16, p. 2480–2498, https:// doi.org/10.1002/2015GC005852.

- Planke, S., Symonds, P.A., Alvestad, E., and Skogseid, J., 2000, Seismic volcanostratigraphy of large-volume basaltic extrusive complexes on rifted margins: Journal of Geophysical Research: Solid Earth, v. 105, p. 19,335–19,351, https://doi.org/10.1029/1999JB900005.
- Plaza-Faverola, A., Klaeschen, D., Barnes, P., Pecher, I., Henrys, S., and Mountjoy, J., 2012, Evolution of fluid expulsion and concentrated hydrate zones across the southern Hikurangi subduction margin, New Zealand: An analysis from depth migrated seismic data: Geochemistry, Geophysics, Geosystems, v. 13, https://doi.org/10.1029/2012GC004228.
- Plaza-Faverola, A., Henrys, S., Pecher, I., Wallace, L., and Klaeschen, D., 2016, Splay fault branching from the Hikurangi subduction shear zone: Implications for slow slip and fluid flow: Geochemistry, Geophysics, Geosystems, v. 17, p. 5009–5023, https://doi.org /10.1002/2016GC006563.
- Prada, M., Bartolomé, R., Gras, C., Bandy, W.L., and Dañobeitia, J.J., 2023, Trench-parallel ridge subduction controls upper-plate structure and shallow megathrust seismogenesis along the Jalisco-Colima margin, Mexico: Communications Earth & Environment, v. 4, 53, https://doi.org/10.1038/s43247-023-00705-9.
- Rabinowitz, H.S., Savage, H.M., Skarbek, R.M., Ikari, M.J., Carpenter, B.M., and Collettini, C., 2018, Frictional behavior of input sediments to the Hikurangi Trench, New Zealand: Geochemistry, Geophysics, Geosystems, v. 19, p. 2973–2990, https://doi.org/10.1029/2018GC007633.
- Ranero, C.R., and von Huene, R., 2000, Subduction erosion along the Middle America convergent margin: Nature, v. 404, p. 748–752, https://doi.org/10.1038/35008046.
- Ranero, C.R., Phipps Morgan, J., McIntosh, K., and Relchert, C., 2003, Bending-related faulting and mantle serpentinization at the Middle America trench: Nature, v. 425, p. 367–373, https:// doi.org/10.1038/nature01961.
- Ranero, C.R., Villaseñor, A., Morgan, J.P., and Weinrebe, W., 2005, Relationship between bendfaulting at trenches and intermediate-depth seismicity: Geochemistry, Geophysics, Geosystems, v. 6, https://doi.org/10.1029/2005GC000997.
- Reinhard, A.A., Jackson, M.G., Blusztajn, J., Koppers, A.A.P., Simms, A.R., and Konter, J.G., 2019, "Petit spot" rejuvenated volcanism superimposed on plume-derived Samoan shield volcanoes: Evidence from a 645-m drill core from Tutuila Island, American Samoa: Geochemistry, Geophysics, Geosystems, v. 20, p. 1485–1507, https://doi.org/10.1029/2018GC007985.
- Reyners, M., Eberhart-Phillips, D., and Bannister, S., 2017, Subducting an old subduction zone sideways provides insights into what controls plate coupling: Earth and Planetary Science Letters, v. 466, p. 53–61, https://doi.org/10.1016/j.epsl.2017.03.004.
- Riefstahl, F., Gohl, K., Davy, B., and Barrett, R., 2020a, Extent and cessation of the Mid-Cretaceous Hikurangi Plateau underthrusting: Impact on global plate tectonics and the submarine Chatham Rise: Journal of Geophysical Research: Solid Earth, v. 125, https://doi.org/10.1029/2020JB019681.
- Riefstahl, F., Gohl, K., Davy, B., Hoernle, K., Mortimer, N., Timm, C., Werner, R., and Hochmuth, K., 2020b, Cretaceous intracontinental rifting at the southern Chatham Rise margin and initialisation of seafloor spreading between Zealandia and Antarctica: Tectonophysics, v. 776, https://doi.org/10.1016/j.tecto.2019.228298.
- Riel, N., Duarte, J.C., Almeida, J., Kaus, B.J.P., Rosas, F., Rojas-Agramonte, Y., and Popov, A., 2023, Subduction initiation triggered the Caribbean large igneous province: Nature Communications, v. 14, 786, https://doi.org/10.1038/s41467-023-36419-x.
- Roberge, J., Wallace, P.J., White, R.V., and Coffin, M.F., 2005, Anomalous uplift and subsidence of the Ontong Java Plateau inferred from CO₂ contents of submarine basaltic glasses: Geology, v. 33, p. 501–504, https://doi.org/10.1130/G21142.1.
- Rogers, G.C., 1982, Oceanic plateaus as meteorite impact signatures: Nature, v. 299, p. 341–342, https://doi.org/10.1038/299341a0.
- Ruh, J.B., Sallarès, V., Ranero, C.R., and Gerya, T., 2016, Crustal deformation dynamics and stress evolution during seamount subduction: High-resolution 3-D numerical modeling: Journal of Geophysical Research: Solid Earth, v. 121, p. 6880–6902, https://doi .org/10.1002/2016JB013250.
- Saffer, D.M., and Tobin, H.J., 2011, Hydrogeology and mechanics of subduction zone forearcs: Fluid flow and pore pressure: Annual Review of Earth and Planetary Sciences, v. 39, p. 157–186, https://doi.org/10.1146/annurev-earth-040610-133408.
- Saffer, D.M., and Wallace, L.M., 2015, The frictional, hydrologic, metamorphic and thermal habitat of shallow slow earthquakes: Nature Geoscience, v. 8, p. 594–600, https://doi.org/10.1038/ngeo2490.
- Sage, F., Collot, J.-Y., and Ranero, C.R., 2006, Interplate patchiness and subduction-erosion mechanisms: Evidence from depth-migrated seismic images at the central Ecuador convergent margin: Geology, v. 34, p. 997–1000, https://doi.org/10.1130/G22790A.1.

- Sager, W.W., Zhang, J., Korenaga, J., Sano, T., Koppers, A.A.P., Widdowson, M., and Mahoney, J.J., 2013, An immense shield volcano within the Shatsky Rise oceanic plateau, northwest Pacific Ocean: Nature Geoscience, v. 6, p. 976–981, https://doi.org/10.1038/ngeo1934.
- Sano, T., Shirao, M., Tani, K., Tsutsumi, Y., Kiyokawa, S., and Fujii, T., 2016, Progressive enrichment of arc magmas caused by the subduction of seamounts under Nishinoshima volcano, Izu-Bonin Arc, Japan: Journal of Volcanology and Geothermal Research, v. 319, p. 52-65, https://doi.org/10.1016/j.jvolgeores.2016.03.004.
- Scherwath, M., et al., 2010, Fore-arc deformation and underplating at the northern Hikurangi margin, New Zealand: Journal of Geophysical Research: Solid Earth, v. 115, p. 1–23, https://doi.org/10.1029/2009JB006645.
- Scholz, C.H., 1988, The critical slip distance for seismic faulting: Nature, v. 336, p. 761–763, https://doi.org/10.1038/336761a0.
- Scholz, C.H., 1998, Earthquakes and friction laws: Nature, v. 391, p. 37-42, https://doi.org/10.1038/34097.
- Scholz, C.H., and Small, C., 1997, The effect of seamount subduction on seismic coupling: Geology, v. 25, p. 487–490, https://doi.org/10.1130/0091-7613(1997)025<0487:TEOSSO>2.3.CO;2.
- Schwartz, D.M., Wanless, V.D., Soule, S.A., Schmitz, M.D., and Kurz, M.D., 2020, Monogenetic near-island seamounts in the Galápagos Archipelago: Geochemistry, Geophysics, Geosystems, v. 21, p. 1–30, https://doi.org/10.1029/2020GC008914.
- Scuderi, M.M., Collettini, C., Viti, C., Tinti, E., and Marone, C., 2017, Evolution of shear fabric in granular fault gouge from stable sliding to stick slip and implications for fault slip mode: Geology, v. 45, p. 731–734, https://doi.org/10.1130/G39033.1.
- Self, S., Thordarson, T., and Keszthelyi, L., 2013, Emplacement of continental flood basalt lava flows, in Mahoney, J.J., and Coffin, M.F., eds., Large Igneous Provinces: Continental, Oceanic, and Planetary Flood Volcanism: American Geophysical Union, Geophysical Monograph Series, v. 100. p. 381–410. https://doi.org/10.1029/GM1000381.
- Shaddox, H.R., and Schwartz, S.Y., 2019, Subducted seamount diverts shallow slow slip to the forearc of the northern Hikurangi subduction zone, New Zealand: Geology, v. 47, p. 415–418, https://doi.org/10.1130/G45810.1.
- Shillington, D.J., Bécel, A., Nedimović, M.R., Kuehn, H., Webb, S.C., Abers, G.A., Keranen, K.M., Li, J., Delescluse, M., and Mattei-Salicrup, G.A., 2015, Link between plate fabric, hydration and subduction zone seismicity in Alaska: Nature Geoscience, v. 8, p. 961–964, https://doi .org/10.1038/ngeo2586.
- Shreedharan, S., Ikari, M., Wood, C., Saffer, D., Wallace, L., and Marone, C., 2022, Frictional and lithological controls on shallow slow slip at the northern Hikurangi margin: Geochemistry, Geophysics, Geosystems, v. 23, p. 1–20, https://doi.org/10.1029/2021GC010107.
- Shreedharan, S., Saffer, D., Wallace, L.M., and Williams, C., 2023, Ultralow frictional healing explains recurring slow slip events: Science, v. 379, p. 712–717, https://doi.org/10.1126/science.adt/030
- Skarbek, R.M., Rempel, A.W., and Schmidt, D.A., 2012, Geologic heterogeneity can produce aseismic slip transients: Geophysical Research Letters, v. 39, p. 1–5, https://doi.org/10.1029/2012GL053762.
- Smith, D.K., and Cann, J.R., 1990, Hundreds of small volcanoes on the median valley floor of the Mid-Atlantic Ridge at 24–30° N: Nature, v. 348, p. 152–155, https://doi.org/10.1038/348152a0.
- Smith, W.H.F., and Sandwell, D.T., 1997, Global sea floor topography from satellite altimetry and ship depth soundings: Science, v. 277, p. 1956–1962, https://doi.org/10.1126/science.277.5334.1956.
- Stern, T., Lamb, S., Moore, J.D.P., Okaya, D., and Hochmuth, K., 2020, High mantle seismic P-wave speeds as a signature for gravitational spreading of superplumes: Science Advances, v. 6, https://doi.org/10.1126/sciadv.aba7118.
- Stern, T.A., Henrys, S.A., Okaya, D., Louie, J.N., Savage, M.K., Lamb, S., Sato, H., Sutherland, R., and Iwasaki, T., 2015, A seismic reflection image for the base of a tectonic plate: Nature, v. 518, p. 85–88, https://doi.org/10.1038/nature14146.
- Sun, T., Saffer, D., and Ellis, S., 2020, Mechanical and hydrological effects of seamount subduction on megathrust stress and slip: Nature Geoscience, v. 13, p. 249–255, https://doi.org/10.1038/s41561-020-0542-0.
- Tan, H., Gao, X., Wang, K., Gao, J., and He, J., 2022, Hidden roughness of subducting seafloor and implications for megathrust seismogenesis: Example from northern Manila Trench: Geophysical Research Letters, v. 49, https://doi.org/10.1029/2022GL100146.
- Tarduno, J.A., Sliter, W.V., Kroenke, L., Lickie, M., Mayer, H., Mahoney, J.J., Musgrave, R., Storey, M., and Winterer, E.L., 1991, Rapid formation of Ontong Java Plateau by Aptian mantle plume volcanism: Science, v. 254, p. 399–403, https://doi.org/10.1126/science.254.5030.399.

- Taylor, B., 2006, The single largest oceanic plateau: Ontong Java–Manihiki–Hikurangi: Earth and Planetary Science Letters, v. 241, p. 372–380, https://doi.org/10.1016/j.epsl 2005 11 049
- Tejada, M.L.G., 2002, Basement geochemistry and geochronology of central Malaita, Solomon Islands, with implications for the origin and evolution of the Ontong Java Plateau: Journal of Petrology, v. 43, p. 449–484, https://doi.org/10.1093/petrology/43.3.449.
- Tejada, M.L.G., Mahoney, J.J., Duncan, R.A., and Hawkins, M.P., 1996, Age and geochemistry of basement and alkalic rocks of Malaita and Santa Isabel, Solomon Islands, southern margin of Ontong Java Plateau: Journal of Petrology, v. 37, p. 361–394, https://doi.org/10.1093 /petrology/37.2.361.
- Thomson, K., and Schofield, N., 2008, Lithological and structural controls on the emplacement and morphology of sills in sedimentary basins, in Thomson, K., and Petford, N., eds., Structure and Emplacement of High-Level Magmatic Systems: Geological Society, London, Special Publication 302, p. 31–44, https://doi.org/10.1144/SP302.3.
- Thordarson, T., 2004, Accretionary-lapilli-bearing pyroclastic rocks at ODP Leg 192 Site 1184: A record of subaerial phreatomagmatic eruptions on the Ontong Java Plateau, in Fitton, J.G., Mahoney, J.J., Wallace, P.J., and Saunders, A.D., eds., Origin and Evolution of the Ontong Java Plateau: Geological Society, London, Special Publication 229, p. 275–306, https://doi.org/10.1144/GSL.SP.2004.229.01.16.
- Timm, C., Hoernle, K., Werner, R., Hauff, F., den Bogaard, P., van White, J., Mortimer, N., and Garbe-Schönberg, D., 2010, Temporal and geochemical evolution of the Cenozoic intraplate volcanism of Zealandia: Earth-Science Reviews, v. 98, p. 38–64, https://doi.org/10.1016/j .earscirev.2009.10.002.
- Timm, C., Hoernle, K., Werner, R., Hauff, F., den Bogaard, P., van Michael, P., Coffin, M.F., and Koppers, A., 2011, Age and geochemistry of the oceanic Manihiki Plateau, SW Pacific: New evidence for a plume origin: Earth and Planetary Science Letters, v. 304, p. 135–146, https:// doi.org/10.1016/j.epsl.2011.01.025.
- Timm, C., Bassett, D., Graham, I.J., Leybourne, M.I., de Ronde, C.E.J., Woodhead, J., Layton-Matthews, D., and Watts, A.B., 2013, Louisville Seamount subduction and its implication on mantle flow beneath the central Tonga-Kermadec arc: Nature Communications, v. 4, 1720, https://doi.org/10.1038/ncomms2702.
- Timm, C., et al., 2014, Subduction of the oceanic Hikurangi Plateau and its impact on the Kermadec arc: Nature Communications, v. 5, 4923, https://doi.org/10.1038/ncomms5923.
- Todd, E.K., and Schwartz, S.Y., 2016, Tectonic tremor along the northern Hikurangi margin, New Zealand, between 2010 and 2015: Journal of Geophysical Research: Solid Earth, v. 121, p. 8706– 8719, https://doi.org/10.1002/2016JB013480.
- Todd, E.K., et al., 2018, Earthquakes and tremor linked to seamount subduction during shallow slow slip at the Hikurangi margin, New Zealand: Journal of Geophysical Research: Solid Earth, v. 123, p. 6769–6783, https://doi.org/10.1029/2018JB016136.
- Tonegawa, T., et al., 2019, Characterization of crustal and uppermost-mantle seismic discontinuities in the Ontong Java Plateau: Journal of Geophysical Research: Solid Earth, v. 124, p. 7155–7170, https://doi.org/10.1029/2018JB016970.
- Tozer, B., Sandwell, D.T., Smith, W.H.F., Olson, C., Beale, J.R., and Wessel, P., 2019, Global bathymetry and topography at 15 arc sec: SRTM15+: Earth and Space Science, v. 6, p. 1847–1864, https://doi.org/10.1029/2019EA000658.
- Underwood, M.B., 2021, Data report: Clay mineral assemblages within biocalcareous and volcaniclastic inputs to the Hikurangi subduction zone, IODP Expedition 372B/375 Sites U1520 and U1526, offshore New Zealand: Proceedings of the International Ocean Discovery Program, v. 372/375, https://doi.org/10.14379/jodp.proc.372B375.2072021.
- Valentine, G.A., and Hirano, N., 2010, Mechanisms of low-flux intraplate volcanic fields—Basin and Range (North America) and northwest Pacific Ocean: Geology, v. 38, p. 55–58, https://doi.org/10.1130/G30427.1.
- Van Avendonk, H.J.A., Holbrook, W.S., Lizarralde, D., and Denyer, P., 2011, Structure and serpentinization of the subducting Cocos Plate offshore Nicaragua and Costa Rica: Geochemistry, Geophysics, Geosystems, v. 12, https://doi.org/10.1029/2011GC003592.
- Van Avendonk, H.J.A., Davis, J.K., Harding, J.L., and Lawver, L.A., 2017, Decrease in oceanic crustal thickness since the breakup of Pangaea: Nature Geoscience, v. 10, p. 58–61, https:// doi.org/10.1038/ngeo2849.
- van de Lagemaat, S.H.A., Kamp, P.J.J., Boschman, L.M., and van Hinsbergen, D.J.J., 2023, Reconciling the Cretaceous breakup and demise of the Phoenix Plate with East Gondwana orogenesis in New Zealand: Earth-Science Reviews, v. 236, https://doi.org/10.1016/j .earscirev.2022.104276.

- von Huene, R., Reston, T., Kukwski, N., Dehghani, G., and Weinrebe, W., 1997, A subducting seamount beneath the Mediterranean Ridge: Tectonophysics, v. 271, p. 249–261, https://doi.org/10.1016/S0040-1951(96)00241-7.
- von Huene, R., Ranero, C.R., and Vannucchi, P., 2004, Generic model of subduction erosion: Geology, v. 32, p. 913–916, https://doi.org/10.1130/G20563.1.
- Wallace, L.M., 2020, Slow slip events in New Zealand: Annual Review of Earth and Planetary Sciences, v. 48, p. 175–203, https://doi.org/10.1146/annurev-earth-071719-055104.
- Wallace, L.M., Beavan, J., McCaffrey, R., and Darby, D., 2004, Subduction zone coupling and tectonic block rotations in the North Island, New Zealand: Journal of Geophysical Research: Solid Earth, v. 109, p. 1–21, https://doi.org/10.1029/2004JB003241.
- Wallace, L.M., McCaffrey, R., Beavan, J., and Ellis, S., 2005, Rapid microplate rotations and backarc rifting at the transition between collision and subduction: Geology, v. 33, p. 857–860, https:// doi.org/10.1130/G21834.1.
- Wallace, L.M., et al., 2009, Characterizing the seismogenic zone of a major plate boundary subduction thrust: Hikurangi margin, New Zealand: Geochemistry, Geophysics, Geosystems, v. 10, https://doi.org/10.1029/2009GC002610.
- Wallace, L.M., Fagereng, A., and Ellis, S., 2012, Upper plate tectonic stress state may influence interseismic coupling on subduction megathrusts: Geology, v. 40, p. 895–898, https://doi.org/10.1130/G33373.1.
- Wallace, L.M., Webb, S.C., Ito, Y., Mochizuki, K., Hino, R., Henrys, S., Schwartz, S.Y., and Sheehan, A.F., 2016, Slow slip near the trench at the Hikurangi subduction zone, New Zealand: Science, v. 352. p. 701–704. https://doi.org/10.1126/science.aaf2349.
- Wallace, L.M., et al., 2019, Site U1526: Proceedings of the International Ocean Discovery Program 372B/375, https://doi.org/10.14379/iodp.proc.372B375.106.2019.
- Walther, C.H.E., 2003, The crustal structure of the Cocos Ridge off Costa Rica: Journal of Geophysical Research: Solid Earth, v. 108, https://doi.org/10.1029/2001JB000888.
- Wang, K., and Bilek, S.L., 2011, Do subducting seamounts generate or stop large earthquakes?: Geology, v. 39, p. 819–822, https://doi.org/10.1130/G31856.1.
- Wang, K., and Bilek, S.L., 2014, Invited review paper: Fault creep caused by subduction of rough seafloor relief: Tectonophysics, v. 610, p. 1–24, https://doi.org/10.1016/j.tecto.2013.11.024.
- Wang, M., et al., 2023, Compactive deformation of incoming calcareous pelagic sediments, northern Hikurangi subduction margin, New Zealand: Implications for subduction processes: Earth and Planetary Science Letters, v. 605, https://doi.org/10.1016/j.epsl.2023.118022.
- Warren-Smith, E., Fry, B., Wallace, L., Chon, E., Henrys, S., Sheehan, A., Mochizuki, K., Schwartz, S., Webb, S., and Lebedev, S., 2019, Episodic stress and fluid pressure cycling in subducting oceanic crust during slow slip: Nature Geoscience, v. 12, p. 475–481, https://doi.org/10.1038/s41561-019-0367-x.
- Wells, R., Bukry, D., Friedman, R., Pyle, D., Duncan, R., Haeussler, P., and Wooden, J., 2014, Geologic history of Siletzia, a large igneous province in the Oregon and Washington Coast Range: Correlation to the geomagnetic polarity time scale and implications for a long-lived Yellowstone hotspot: Geosphere, v. 10, p. 692–719, https://doi.org/10.1130 /GES01018.1.
- Wessel, P., Luis, J.F., Uieda, L., Scharroo, R., Wobbe, F., Smith, W.H.F., and Tian, D., 2019, The Generic Mapping Tools Version 6: Geochemistry, Geophysics, Geosystems, v. 20, p. 5556–5564, https://doi.org/10.1029/2019GC008515.
- White, J.D.L., Schipper, C.I., and Kano, K., 2015, Submarine explosive eruptions, *in* The Encyclopedia of Volcanoes: Elsevier, p. 553–569, https://doi.org/10.1016/B978-0-12-385938 -9.00031-6.
- White, R.S., McKenzie, D., and O'Nions, R.K., 1992, Oceanic crustal thickness from seismic measurements and rare earth element inversions: Journal of Geophysical Research: Solid Earth, v. 97, p. 19,683–19,715, https://doi.org/10.1029/92JB01749.
- White, R.V., Castillo, P.R., Neal, C.R., Fitton, J.G., and Godard, M., 2004, Phreatomagmatic eruptions on the Ontong Java Plateau: Chemical and isotopic relationship to Ontong Java Plateau basalts, in Fitton, J.G., Mahoney, J.J., Wallace, P.J., and Saunders, A.D., eds., Origin and Evolution of the Ontong Java Plateau: Geological Society, London, Special Publication 229, p. 307–323, https://doi.org/10.1144/GSL.SP.2004.229.01.17.
- Williams, C.A., Eberhart-Phillips, D., Bannister, S., Barker, D.H.N., Henrys, S., Reyners, M., and Sutherland, R., 2013, Revised interface geometry for the Hikurangi subduction zone, New Zealand: Seismological Research Letters, v. 84, p. 1066–1073, https://doi.org/10 .1785/0220130035.
- Wood, R., and Davy, B., 1994, The Hikurangi Plateau: Marine Geology, v. 118, p. 153–173, https://doi.org/10.1016/0025-3227(94)90118-X.

- Woods, K., et al., 2022, Using seafloor geodesy to detect vertical deformation at the Hikurangi subduction zone: Insights from self-calibrating pressure sensors and ocean general circulation models: Journal of Geophysical Research: Solid Earth, v. 127, https://doi.org/10.1029/2022JB023989.
- Worthington, L.L., Van Avendonk, H.J.A., Gulick, S.P.S., Christeson, G.L., and Pavlis, T.L., 2012, Crustal structure of the Yakutat terrane and the evolution of subduction and collision in southern Alaska: Journal of Geophysical Research: Solid Earth, v. 117, https://doi.org/10 .1029/2011JB008493.
- Yang, J., and Faccenda, M., 2020, Intraplate volcanism originating from upwelling hydrous mantle transition zone: Nature, v. 579, p. 88–91, https://doi.org/10.1038/s41586-020-2045-y.
- Yarce, J., et al., 2019, Seismicity at the northern Hikurangi margin, New Zealand, and investigation of the potential spatial and temporal relationships with a shallow slow slip

- event: Journal of Geophysical Research: Solid Earth, v. 124, p. 4751–4766, https://doi.org/10.1029/2018JB017211.
- Zeumann, S., and Hampel, A., 2015, Deformation of erosive and accretive forearcs during subduction of migrating and non-migrating aseismic ridges: Results from 3-D finite element models and application to the Central American, Peruvian, and Ryukyu margins: Tectonics, v. 34, p. 1769–1791, https://doi.org/10.1002/2015TC003867.
- Zhang, J., Sager, W.W., and Korenaga, J., 2015, The Shatsky Rise oceanic plateau structure from two-dimensional multichannel seismic reflection profiles and implications for oceanic plateau formation, in Neal, C.R., Sager, W.W., Sano, T., and Erba, E., The Origin, Evolution, and Environmental Impact of Oceanic Large Igneous Provinces: Geological Society of America Special Paper 511, p. 103–126, https://doi.org/10.1130/2015.2511(06).